ARTICLE

Reactions of [(dmpe)$_2$MnH(C$_2$H$_4$)] with Hydrogermanes to Form Germylene, Germyl, Hydrogermane, and Germanide Complexes

Received 00th January 20xx,
Accepted 00th January 20xx

DOI: 10.1039/x0xx00000x

Jeffrey S. Price,[a] Ignacio Vargas-Baca,[a] David J. H. Emslie,*[a] and James F. Britten[b]

Reactions of the ethylene hydride complex *trans*-[(dmpe)$_2$MnH(C$_2$H$_4$)] (**1**) with secondary hydrogermanes H$_2$GeR$_2$ at 55-60 °C afforded the base-free terminal germylene hydride complexes *trans*-[(dmpe)$_2$MnH(=GeR$_2$)] (R = Ph; **2a**, R = Et; **2b**). Room temperature reactions of **2a** or **2b** with an excess of the primary hydrogermanes H$_3$GeR' (R' = Ph or ^{n}Bu) afforded *trans*-[(dmpe)$_2$MnH(=GeHR')] (R' = Ph; **3a**, R' = ^{n}Bu; **3b**) in rapid eqilibrium with small amounts of **2a/b**, as well as the digermyl hydride complex *mer*-[(dmpe)$_2$MnH(GeH$_2$R')$_2$] {R' = Ph (**4a**) or ^{n}Bu (**4b**)} and the *trans*-hydrogermane germyl complex *trans*-[(dmpe)$_2$Mn(GeH$_2$R')(HGeH$_2$R')] {R' = Ph (**5a**) or ^{n}Bu (**5b**)}. Pure **3b** was isolated from the reaction of **2b** with H$_3$Ge^{n}Bu, whereas **3a** decomposed readily in solution in the absence of free H$_3$GePh, and a pure bulk sample was not obtained. Reactions of **1** with H$_3$GeR' (R' = Ph or ^{n}Bu) also proceeded at 55-60 °C to afford mixtures of **3a/b**, **4a/b** and **5a/b**, accompanied by remaining **1**. However, upon continued heating to consume **1**, various unidentified manganese-containing intermediates were formed, ultimately affording the germanide complex [{(dmpe)$_2$MnH}$_2$(μ-Ge)] (**6**) in 30-45% spectroscopic yield. Pure ***trans,trans*-6** was isolated in 28% yield from the reaction of **1** with H$_3$Ge^{n}Bu, and it is notable that this reaction involves stripping of all four substituents from the hydrogermane. Complexes **2a**, **3a**, and **6** were crystallographically characterized, and the nature of the Mn=Ge bonding in these species (as well as in **2b** and **3b**) was probed computationally.

Introduction

In 1963, Stone and co-workers published the spectroscopic observation of the first manganese germylene complex, [{(OC)$_5$Mn}$_2$(μ-GeH$_2$)], obtained by the reaction of GeH$_4$ with either [HMn(CO)$_5$] or (in significantly lower yield) [Mn$_2$(CO)$_{10}$].[1] However, despite the intervening 60 years, all isolated manganese germylene complexes feature bridging[1-15] or base-coordinated[10,16-20] germylene ligands in which germanium is 4-coordinate or higher. As a consequence, these complexes exhibit diminished Mn–Ge multiple bond character; those for which an X-ray crystal structure was obtained (**I**-**VIII** in Figure 1)[8,10,12,14,15,17-19] feature Mn–Ge distances of 2.32-2.42 Å (terminal GeR$_2$L compounds) and 2.36-2.60 Å (μ-GeR$_2$ compounds). These distances are similar to those for crystallographically characterized manganese germyl complexes (Mn–Ge = 2.29-2.47 Å for GeX$_3$ (X = halide or H) compounds[21-25] and 2.41-2.54 Å for other germyl compounds[19,26-28]), although direct comparisons are hampered by differences in the substituents on germanium. By contrast, a significantly shorter Mn–Ge distance of 2.236(1) Å was reported for [{(Me$_3$SiN=PPh$_2$)$_2$C=Ge}Mn(CO)$_2$Cp] (**IX** in Figure 1). This complex features trigonal planar germanium, and was described as an imine-stabilized germavinylidene complex based on the very short Ge–C distance of 1.885(3) Å.[29]

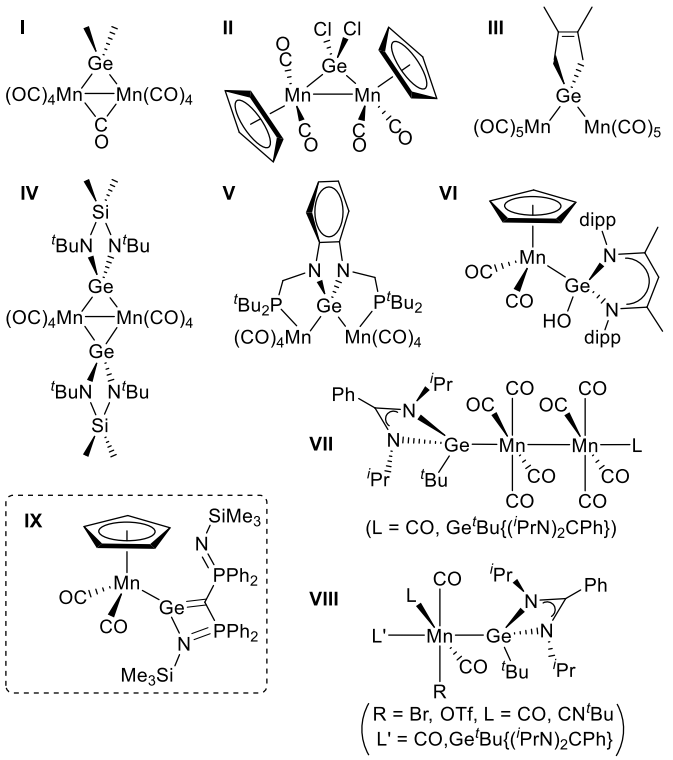

Figure 1. Crystallographically characterized manganese germylene[8,10,12,14,15,17-19] and (in the inset) germavinylidene[29] complexes.

[a.] *Department of Chemistry, McMaster University, 1280 Main St. West, Hamilton, Ontario, L8S 4M1. E-mail: emslied@mcmaster.ca.*
[b.] *McMaster Analytical X-ray Diffraction Facility (MAX), McMaster University, 1280 Main St. West, Hamilton, Ontario, L8S 4M1.*

Electronic Supplementary Information (ESI) available: selected NMR spectra, SCD and PXRD data, and DFT results. CCDC 2284213-2284216. For ESI and crystallographic data in CIF or other electronic format see DOI: 10.1039/x0xx00000x

Short Mn–Ge distances have also been reported for manganese germanide complexes. In the 1980s, the Weiss and Herrmann groups published a family of complexes that were described as featuring zero-valent Ge atoms sandwiched between $^{R}CpMn(CO)_2$ fragments (^{R}Cp = C_5H_5, C_5H_4Me or C_5Me_5; **X**-**XI** in Figure 2).[30-32] X-ray crystal structures of these complexes revealed Mn–Ge bond distances of 2.18-2.26 Å, consistent with substantial multiple-bond character. This was confirmed by calculations by Fenske and Hall, which indicated that the Mn–Ge bonds can best be described as 'partial triple bonds' (with a bond order of two) rather than localized double bonds, given that the 3-atom π system features roughly cylindrical symmetry.[33] Consequently, the bonding description for the Mn=Ge=Mn core of a μ_2-germanide compound differs significantly from that of an allene ($R_2C=C=CR_2$). The only other crystallographically characterized μ_2-germanide complex is [{CpRe(κ²-nacnac)}₂(μ-Ge)] (nacnac = CH{CMeN(Dipp)}₂),[34] containing an M–Ge–M angle (163.18(2)°) that is significantly perturbed from linearity (cf. 179(1)-180° in the dimanganese complexes in Figure 2). A handful of transition metal μ_2-silicide complexes have recently been reported.[35,36]

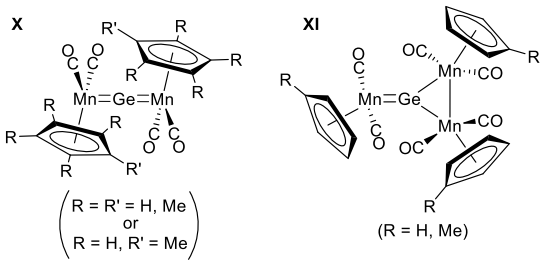

Figure 2. Zero-valent germanium complexes featuring Mn=Ge double bonds reported by Weiss or Herrmann. All species were crystallographically characterized except [{CpMn(CO)₂}₂(μ-Ge)].[30-32]

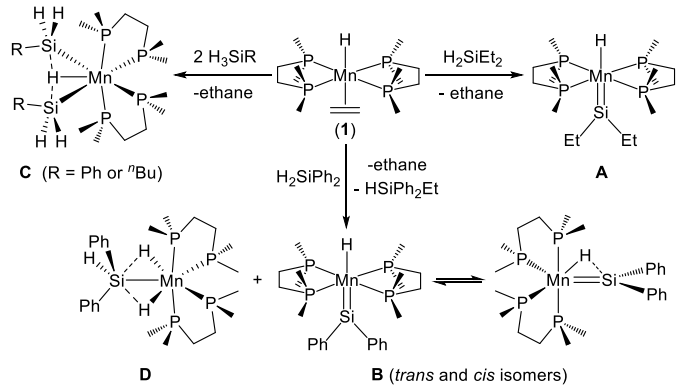

Scheme 1. Reactions of $[(dmpe)_2MnH(C_2H_4)]$ (**1**) with hydrosilanes.[37,38] Only one isomer of $[(dmpe)_2MnH_2(SiHPh_2)]$ (**D**) is shown.

Our group previously described reactions between $[(dmpe)_2MnH(C_2H_4)]$ (**1**) and hydrosilanes to afford manganese silylene ($[(dmpe)_2MnH(=SiR_2)]$; R = Et, Ph; **A**-**B** in Scheme 1) complexes and disilyl hydride ($[(dmpe)_2MnH(SiH_2R)_2]$; R = Ph, ^{n}Bu) complexes (**C** in Scheme 1; when H_2SiPh_2 was used, $[(dmpe)_2MnH_2(SiHPh_2)]$ (**D**) was also generated).[37,38] The dialkylsilylene complex $[(dmpe)_2MnH(=SiEt_2)]$ (**A**) was observed exclusively as the *trans* isomer in solution and the solid state, whereas $[(dmpe)_2MnH(=SiPh_2)]$ (**B**) exists in solution as an equilibrium mixture of a *cis* and a *trans* isomer (with and without an interligand Si–H interaction, respectively), the former of which preferentially crystallized.

In this work we report reactions of **1** with hydrogermanes, with a view towards accessing the first manganese complexes of planar (i.e. base-free) terminal germylene ligands, and more generally, to probe the similarities and differences in the reactivity of **1** with hydrogermanes versus hydrosilanes. These reactions led to the formation of germylene, germyl, hydrogermane and germanide complexes.

Results and discussion

Reactions of *trans*-$[(dmpe)_2MnH(C_2H_4)]$ (1) with Hydrogermanes

The manganese(I) ethylene hydride complex *trans*-$[(dmpe)_2MnH(C_2H_4)]$ (**1**)[39,40] reacted with an excess of secondary hydrogermanes H_2GeR_2 (R = Ph, Et) at 55-60 °C to afford dark red or red-brown germylene hydride complexes *trans*-$[(dmpe)_2MnH(=GeR_2)]$ (**2a**; R = Ph, **2b**; R = Et) and ethane; Scheme 2. Complexes **2a**-**b** gave rise to a single ^{31}P NMR resonance (**2a**; 79.7 ppm, **2b**; 79.9 ppm), as well as four dmpe alkyl environments and a low frequency hydride signal (**2a**; –10.02 ppm, **2b**; –10.79 ppm) in the ^{1}H NMR spectra, together characteristic of C_{2v}-symmetric *trans* germylene hydride complexes. The Mn*H* environments appear as quintets with $^{2}J_{P,H}$ coupling of 52-56 Hz, which is very similar to those observed for the silylene analogues (51-55 Hz for **A** and *trans*-**B** in Scheme 1)[37] and complex **1** (57 Hz).[40] Compounds **2a**-**b** demonstrate appreciable thermal stability, with negligible decomposition after 3 days in C_6D_6 at 80 °C.

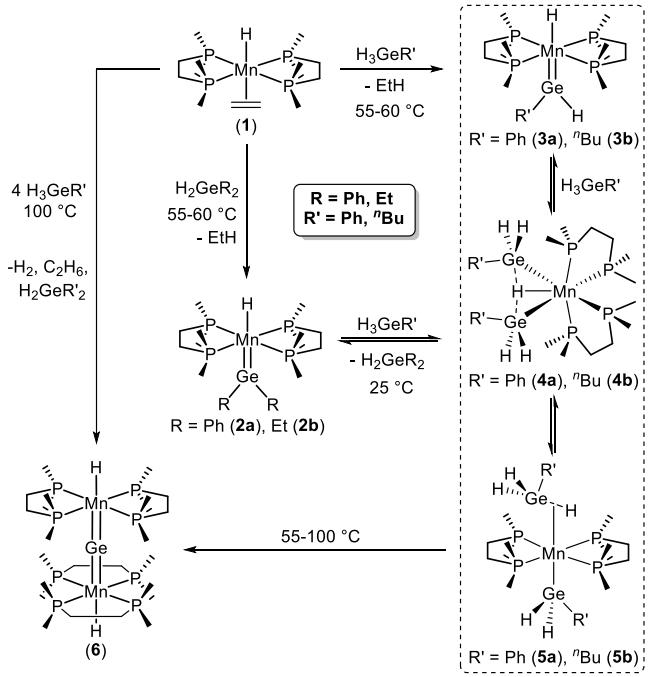

Scheme 2. Reactions of $[(dmpe)_2MnH(C_2H_4)]$ (**1**) with hydrogermanes to afford $[(dmpe)_2MnH(=GeR_2)]$ (**2a**: R= Ph, **2b**: R = Et), $[(dmpe)_2MnH(=GeHR')]$ (**3a**: R′ = Ph, **3b**: R′ = ^{n}Bu), *mer*-$[(dmpe)_2MnH(GeH_2R')_2]$ (**4a**; R′ = Ph, **4b**; R′ = ^{n}Bu), *trans*-

[(dmpe)$_2$Mn(GeH$_2$R')(HGeH$_2$R')] (**5a**; R' = Ph, **5b**; R' = ^{n}Bu), and [{(dmpe)$_2$MnH}$_2$(μ-Ge)] (**6**). Only one isomer of **6** is shown.

An X-ray crystal structure was obtained for the diphenylgermylene complex [(dmpe)$_2$MnH(=GePh$_2$)] (**2a**; a in Figure 3), revealing *trans*-disposed germylene and hydride ligands, and an equatorial belt of two dmpe ligands completing an octahedral coordination environment, consistent with the solution structures of **2a-b** (*vide supra*). As expected for a germylene ligand, the environment at the Ge atom is trigonal planar {Σ(X–Mn–Y) = 360.00(8)°} and the Mn–Ge distance of 2.2636(4) Å is shorter than that in previously reported manganese germyl complexes (2.29-2.54 Å). This distance lies at the upper end of the range for previously reported manganese complexes where the Mn–Ge bond displays appreciable double bond character (2.18-2.26 Å; *vide infra*).

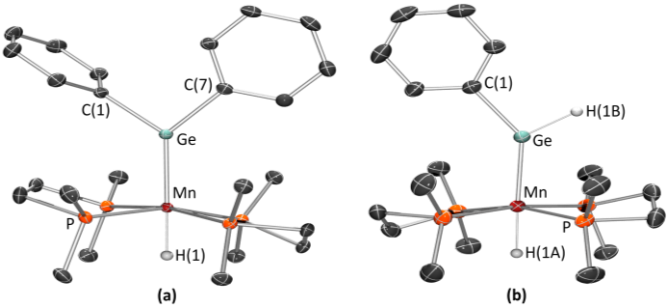

Figure 3. X-ray crystal structures of (a) [(dmpe)$_2$MnH(=GePh$_2$)] (**2a**) and (b) [(dmpe)$_2$MnH(=GeHPh)] (**3a**), with ellipsoids at 50 % probability. Most hydrogen atoms have been omitted for clarity. Hydrogen atoms on Mn and Ge were located from the difference map and refined isotropically. For **2a**, distances (Å) and angles (deg): Mn–Ge 2.2636(4), Mn–H(1) 1.50(2), Ge–C(1) 2.009(1), Ge–C(7) 2.007(1), H(1)–Mn–Ge 178.5(9), Mn–Ge–C(1) 128.68(4), Mn–Ge–C(7) 135.28(4), C(1)–Mn–C(7) 96.04(6), ΣX–Mn–Y 360.00(8). For **3a**, distances (Å) and angles (deg): Mn–Ge 2.2462(6), Mn–H(1A) 1.54(2), Ge–C(1) 1.993(2), Ge–H(1B) 1.54(3), H(1A)–Mn–Ge 177.5(8), Mn–Ge–C(1) 140.22(5), Mn–Ge–H(1B) 124(1), C(1)–Mn–H(1B) 96(1), ΣX–Mn–Y 360(1).

Presumably, the mechanism for the synthesis of **2a-b** is equivalent to that for the reaction of **1** with hydrosilanes (to afford silylene hydride complexes):[37] (i) initial isomerization of **1** to place the ethylene and hydride ligands *cis* to one another, (ii) insertion of the ethylene ligand into the Mn–H bond to afford a 5-coordinate Mn(I) ethyl species, [(dmpe)$_2$MnEt],[38] (iii) reaction with H$_2$GeR$_2$ (via σ-bond metathesis, or oxidative addition followed by C–H bond-forming reductive elimination) to yield a germyl intermediate, [(dmpe)$_2$Mn(GeHR$_2$)], and ethane (the only spectroscopically-observed byproduct), and finally (iv) α-hydride elimination.

In contrast to the aforementioned reactivity of **1** with secondary hydrogermanes, which proceeded cleanly to afford **2a-b**, attempts to synthesize germylene hydride derivatives with one hydrocarbyl and one hydrogen substituent on germanium, [(dmpe)$_2$MnH(=GeHR')] {R' = Ph (**3a**) or ^{n}Bu (**3b**)}, via an analogous route (using H$_3$GePh or H$_3$Ge^{n}Bu in place of H$_2$GeR$_2$) afforded multiple products. After 1 hour at 60 °C, significant **1** still remained, and the dominant new manganese-containing species in solution was the target Ge*H*-containing germylene hydride complex (**3a** or **3b**). However, this was accompanied by two compounds (isomers of one another) formed via hydrogermane addition to **3a-b**, which were identified (*vide infra*) as the digermyl hydride complex *mer*-[(dmpe)$_2$MnH(GeH$_2$R')$_2$] (**4a**; R' = Ph, **4b**; R' = ^{n}Bu; major isomer) and the *trans*-hydrogermane germyl complex *trans*-[(dmpe)$_2$Mn(GeH$_2$R')(HGeH$_2$R')] (**5a**; R' = Ph, **5b**; R' = ^{n}Bu; minor isomer); Scheme 2. Furthermore, upon continued heating at 60 °C to consume remaining **1**, these complexes reacted further to afford several new Mn*H*-containing species, ultimately generating the germanide complex [{(dmpe)$_2$MnH}$_2$(μ-Ge)] (**6**) as the dominant manganese complex in solution (*vide infra*). The reaction to form **6** is remarkable since the germanide ligand is formed via elimination of all substituents from the hydrogermane; related reactivity to form a silicide complex was recently reported by Tilley *et al*.[36]

As an alternative route to access the initially targeted hydrogen-substituted germylene complexes **3a-b**, bis(hydrocarbyl)germylene hydride complexes **2a-b** were exposed to excess primary hydrogermane (H$_3$GePh or H$_3$Ge^{n}Bu) at room temperature. This afforded an equilibrium mixture (Scheme 2) consisting of the same three complexes (**3a-b**, **4a-b**, and **5a-b**) initially formed in the reaction between [(dmpe)$_2$MnH(C$_2$H$_4$)] (**1**) and H$_3$GeR at 55-60 °C, accompanied by the germylene starting material (**2a** or **2b**) when only a small excess (e.g. ≤3 equiv.) of H$_3$GeR was employed. Importantly, under these mild conditions (room temperature), further reactivity to form unidentified products or **6** was not observed.

When diethylgermylene complex **2b** was used as the precursor, pure [(dmpe)$_2$MnH(=GeH^{n}Bu)] (**3b**) was isolated by removal of volatiles (solvent, excess primary hydrogermane, and the secondary hydrogermane byproduct) *in vacuo* followed by recrystallization. By contrast, **3a** (R' = Ph) was not isolated in pure form due to decomposition in solution at room temperature in the absence of excess free hydrogermane. Terminal germylene complexes with hydrocarbyl and hydride substituents on Ge have previously been reported for Fe,[41] Cr,[42] Mo,[43,44] W,[45,46] and Ru,[47-49] but these examples (which include species with interactions between the germylene and a hydride co-ligand) are stabilized by very bulky C(SiMe$_3$)$_3$, Trip (Trip = C$_6$H$_2$^{i}Pr$_3$-2,4,6), Mes, 2,6-Trip$_2$C$_6$H$_3$, and ^{t}Bu groups.

X-ray crystal structures were obtained for both **3a** and **3b**, though the latter was severely disordered and suitable only to establish heavy atom connectivity. The key bonding parameters in **3a** (b in Figure 3) are similar to those for diphenyl germylene complex **2a**, with a short Mn–Ge distance of 2.2462(6) Å, and a planar environment about germanium (sum of the angles around Ge = 360(1)°), although the Mn–Ge–C angle in **3a** (140.22(5)°) is expanded relative to those in **2a** (128.68(4)° and 135.28(4)°), presumably to minimize steric hindrance. The NMR spectra of **3a-b** are also similar to those for **2a-b**, featuring Mn*H* ^{1}H NMR signals at –9.18 (**3a**) or –9.82 (**3b**) ppm with $^2J_{H,P}$ couplings of 53-54 Hz, and one ^{31}P{^{1}H} NMR singlet at 78.6 ppm (for both **3a** and **3b**). In addition, germylene Ge*H* signals were observed at 12.68 (**3a**) and 12.38 (**3b**) ppm in the ^{1}H NMR spectra (cf. 10.0-13.3 ppm for terminal Ge*H* environments in previously reported germylene complexes with hydrocarbyl and hydrogen substituents on Ge).[41,42-49]

NMR spectra were obtained for *mer*-[(dmpe)$_2$MnH(GeH$_2$R')$_2$] (**4a**; R' = Ph, **4b**; R' = ^{n}Bu) and *trans*-[(dmpe)$_2$Mn(GeH$_2$R')(HGeH$_2$R')] (**5a**; R' = Ph, **5b**; R' = ^{n}Bu) in the equilibrium mixtures (with **3a-b**) described above, given that these species were not observed in the absence of free H$_3$GeR'. The amount of **3a-b** in these mixtures was significant (>35 %) even in the presence of 2-6 equiv. of H$_3$GeR', though cooling these solutions shifted the equilibrium to favour **4a-b** and **5a-b** (Figure S91).‡ This behaviour contrasts that of the disilyl hydride analogues of **4a-b**, [(dmpe)$_2$MnH(SiH$_2$R')$_2$] (R' = Ph, ^{n}Bu; **C** in Scheme 1), which were the only species observed in solution under ambient conditions (i.e. silicon analogues of **5a-b** and **3a-b** were not detected, including in the absence of free H$_3$SiR'),[38] although the accessibility of the silylene analogues of **3a-b** was demonstrated by high temperature NMR spectroscopy and trapping experiments.[50]

The ^{1}H NMR spectra of the digermyl hydride complexes, *mer*-[(dmpe)$_2$MnH(GeH$_2$R')$_2$] (**4a**; R' = Ph, **4b**; R' = ^{n}Bu), feature a single low frequency Mn*H* environment (**4a**; –11.37 ppm, **4b**; –10.41 ppm) and two diasterotopic Ge*H* environments integrating to two protons each (**4a**; 4.94, 4.93 ppm, **4b**; 4.09, 3.87 ppm), while the ^{31}P{^{1}H} NMR spectra each contain two signals, at 62.1 and 67.9 ppm (**4a**) or 59.4 and 71.9 ppm (**4b**), consistent with a disphenoidal arrangement of the dmpe ligands. These spectroscopic features mirror those for the silicon analogues, [(dmpe)$_2$MnH(SiH$_2$R')$_2$] (R' = Ph, ^{n}Bu; **C** in Scheme 1).[38] Additionally, the $^2J_{H,P}$ coupling constants for the Mn*H* signals (20-23 Hz) are similar to those in the silicon analogues (**C** in Scheme 1; 17-20 Hz),[38] and the ^{31}P{^{1}H} signals are triplets at low temperature with $^2J_{P,P}$ couplings ranging from 25 to 34 Hz.

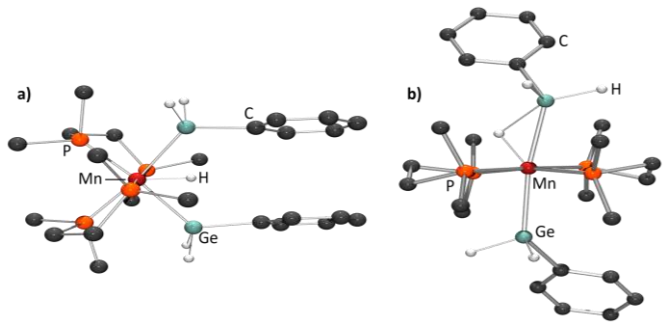

Figure 4. DFT calculated structures (ball and stick diagrams) for the two isomers formed upon H$_3$GePh coordination to [(dmpe)$_2$MnH(=GeHPh)] (**3a**): (a) *mer*-[(dmpe)$_2$MnH(GeH$_2$Ph)$_2$)] (**4a**) and (b) *trans*-[(dmpe)$_2$Mn(GeH$_2$Ph)(HGeH$_2$Ph)] (**5a**). All hydrogen atoms have been omitted for clarity except those on Mn or Ge.

DFT geometry optimization (gas phase, all-electron, TZ2P, PBE, ZORA, D3-BJ) of **4a** (a in Figure 4) and **4b** indicated that these complexes are isostructural with their silicon analogues (**C** in Scheme 1) and feature significant Ge–H interligand interactions. The calculated Ge–H$_{Mn}$ distances of 1.94-1.96 Å are longer than the sum of the covalent radii (1.52 Å) but much shorter than the sum of the van der Waals radii (3.21 Å),[51] with Mayer bond orders ranging from 0.19 to 0.21 (cf. 1.57 Å and 0.86-0.88 for the terminal Ge–H bonds). The significant bonding interactions between the hydride and germyl ligands in the calculated structures of **4a** and **4b** are indicative of incomplete Ge–H bond oxidative addition. The Mn–Ge distances in **4a-b** are 2.48-2.49 Å, and the Mn–H distances are 1.55-1.56 Å.

Hydrogermane-germyl compounds *trans*-[(dmpe)$_2$Mn(GeH$_2$R')(HGeH$_2$R')] (**5a-b**) gave rise to a single sharp ^{31}P{^{1}H} NMR signal (64.9 and 68.0 ppm, respectively), indicative of a complex with two equivalent dmpe ligands lying in a plane. Additionally, a low frequency quintet was observed in the ^{1}H NMR spectra of both **5a** (–11.96 ppm) and **5b** (–12.01 ppm), with $^2J_{H,P}$ coupling (32-33 Hz) that is substantially less than that for the hydride ligand in **1**, **2a-b** and **3a-b**. This is consistent with a manganese-coordinated HGeR$_3$ ligand, and a low frequency quintet with a similarly reduced $^2J_{H,P}$ coupling was observed for the manganese-bound Si*H* proton in *trans*-[(dmpe)$_2$MnH(HSiH$_2$R)] (–12.66 ppm for R = Ph and –13.28 ppm for R = ^{n}Bu, with $^2J_{H,P}$ = 23 Hz in both cases; cf. –10.88 to –11.25 ppm and $^2J_{H,P}$ = 52-54 Hz for the Mn*H* signal).[52] Interestingly, at room temperature, only one terminal GeH environment was observed, whereas at low temperature, two chemically unique terminal Ge*H* environments (integrating to 2H each) were located, arising from the germyl (Ge*H*$_2$R': **5a**; 4.31 ppm, **5b**; 3.29 ppm) and HGeR$_3$ (HGe*H*$_2$R': **5a**; 5.13 ppm, **5b**; 4.29 ppm) ligands.§ These observations point to reversible Ge–H bond oxidative addition (to afford a fluxional 7-coordinate species), which interconverts the GeH$_2$R' and HGeH$_2$R' ligands but does not exchange the terminal and manganese-coordinated Ge*H* groups in the HGeH$_2$R' ligand.

DFT calculations (gas phase, all-electron, TZ2P, PBE, ZORA, D3-BJ) located energy minima corresponding to the *trans*-[(dmpe)$_2$Mn(GeH$_2$R')(HGeH$_2$R')] complexes **5a-b** (for **5a**, see b in Figure 4). The Ge–H bond coordinated to manganese (1.91 Å; Mayer bond order 0.24-0.27) is significantly weakened relative to the terminal Ge–H bonds in the same ligand (1.56-1.57 Å; Mayer bond order 0.85-0.91), consistent with substantial Ge–H bond oxidative addition. This is supported by very similar Mn–Ge distances to the germyl and hydrogermane ligands in **5a-b** (2.48-2.49 Å; the Mn–Ge Mayer bond orders are also very similar (0.70-0.83)), and short Mn–H distances of 1.54-1.55 Å (similar to those calculated for **4a-b**; *vide supra*).¶ These structural attributes mirror those in [(depe)$_2$Mo(CO)(HGeHPh$_2$)] (depe = 1,2-bis(diethylphosphino)ethane), which features (a) a short Mo–Ge distance of 2.6368(7) Å, comparable to that in the germyl hydride isomer [(depe)$_2$MoH(GeH$_2$Ph)(CO)] (2.6693(5) Å), (b) a short Mo–H distance (1.72(6) Å) comparable to that in [(depe)$_2$MoH(GeH$_2$Ph)(CO)] (1.72(4) Å), and (c) a significantly elongated Ge–H distance (2.08(6) Å) relative to a free hydrogermane.[53] Substantially elongated Ge–H bonds (2.13(3) Å) were also observed in the solid state structure of [(nacnac^R)Rh(HGeEt$_3$)$_2$] (nacnac^R = CH(CMeNAr)$_2$ where Ar = C$_6$H$_3$(OMe)$_2$-2,6), with a calculated Ge–H Wiberg bond order of 0.24 for the HGeMe$_3$ analogue.[54]

As described above, reactions of **1** with H$_3$GeR' (R' = Ph or ^{n}Bu) only proceeded at elevated temperature, initially affording a mixture of **1**, **3a-b**, **4a-b** and **5a-b** which underwent further reactivity to generate several unidentified Mn*H* complexes, and ultimately afforded [{(dmpe)$_2$MnH}$_2$(μ-Ge)] (**6**) as the major

product in solution; Scheme 2. Analytically pure samples of **6** were isolated in 28 % yield via the reaction of **1** with 4 equivalents of H_3Ge^nBu at 80-100 °C. Byproducts formed in this reaction include an unidentified insoluble precipitate, ethane, H_2, and $H_2GeR'_2$.[††]

Very large maroon X-ray quality crystals of the *trans*,*trans*-isomer of germanide complex **6** (where the hydride ligand on each of the two octahedral manganese centers is *trans* to germanium; Figure 5) were obtained from hexanes at –30 °C, and 2D PXRD of the bulk solid indicated that this isomer is exclusively formed in the solid state. The environment about the germanium atom is nearly linear (Mn–Ge–Mn = 179.81(2)°), and the short Mn–Ge bond distances {2.2806(7) and 2.2817(7) Å} are indicative of multiple bonding character, although they are not as short as those in **2a** and **3a** {2.2636(4) and 2.2462(6) Å, respectively}, presumably at least in part due to increased steric hindrance in **6**. The two sets of dmpe ligands are rotated ~90° relative to each other about the Mn–Ge–Mn axis resulting in approximate D_{4h} molecular symmetry.

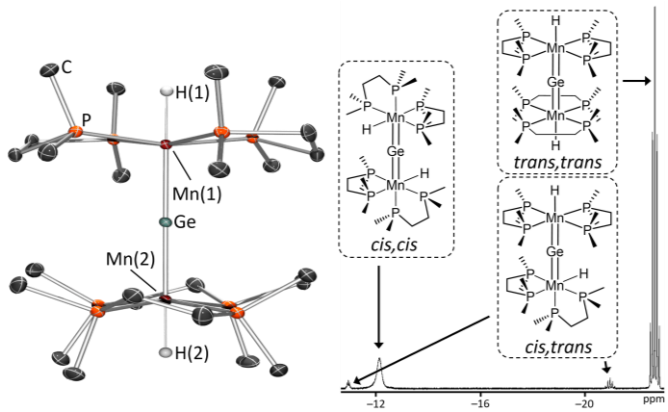

Figure 5. Left; X-ray crystal structure of $[\{(dmpe)_2MnH\}_2(\mu\text{-}Ge)]$ (**6**) with ellipsoids at 50 % probability. Most hydrogen atoms have been omitted for clarity. Hydrogen atoms on Mn were located from the difference map and refined isotropically. Distances (Å) and angles (deg): Mn(1)–Ge 2.2806(7), Mn(2)–Ge 2.2817(7), Mn(1)–H(1) 1.58(3), Mn(2)–H(2) 1.53(3), H(1)–Mn(1)–Ge 180(1), H(2)–Mn(2)–Ge 179(1), Mn(1)–Ge–Mn(2) 179.81(2). Right; Low frequency region of the ^{1}H NMR spectrum of **6** in C_6D_6 showing Mn*H* peaks arising from the three isomers shown in the insets (600 MHz, 298 K).

Upon dissolving pure samples of ***trans*,*trans*-6** in deuterated benzene, three sets of NMR signals were observed (the hydride region of the ^{1}H NMR spectrum is shown in Figure 5) in an 11:5:1 ratio at room temperature. These have been assigned to ***trans*,*trans*-6** (the isomer observed in the solid state), ***cis*,*cis*-6**, and ***cis*,*trans*-6** (Figure 5), and EXSY NMR spectroscopy at elevated temperature indicated that all three isomers are in equilibrium. The hydride region of the ^{1}H NMR spectrum of ***trans*,*trans*-6** features a single quintet at –22.67 ppm with a $^2J_{H,P}$ coupling of 52 Hz, consistent with a hydride ligand adjacent to four equivalent phosphines. By contrast, ***cis*,*trans*-6** gave rise to a pair of Mn*H* signals in the ^{1}H NMR spectrum at 298 K; one quintet with a similar chemical shift and $^2J_{H,P}$ coupling (–20.96 ppm; 53 Hz) to that in ***trans*,*trans*-6**, and another quintet at less negative frequency (–10.93 ppm) with a smaller $^2J_{H,P}$ coupling (24 Hz). At room temperature, ***cis*,*cis*-6** gave rise to a single broad Mn*H* signal at –12.13 ppm, which sharpened somewhat at 334 K (to a afford a broad quintet, or possibly a triplet, in which only the three central peaks are well-resolved) allowing a $^2J_{H,P}$ coupling of 22 Hz to be measured; these data are similar to those for the lower frequency Mn*H* signal for ***cis*,*trans*-6**.

Observation of a ^{1}H NMR quintet for the hydride ligand *cis* to germanium in ***cis*,*trans*-6** at 298 K (and likely also in ***cis*,*cis*-6** at 334 K) is indicative of a fluxional process which renders all phosphine environments on that manganese centre equivalent on the NMR timescale, but does not result in *cis*-*trans* isomerization (because ***cis*,*cis*-6**, ***cis*,*trans*-6** and ***trans*,*trans*-6** do not interconvert rapidly on the NMR timescale at room temperature). This may occur via reversible 1,1-insertion (involving the hydride and germanide ligands; see Scheme S1) to afford a fluxional 5-coordinate manganese centre. Consistent with this explanation, DFT calculations (gas phase, all-electron, TZ2P, PBE, ZORA, D3-BJ) on ***cis*,*trans*-6** and ***cis*,*cis*-6** gave rise (in the lowest energy rotamers) to short Ge···H_{Mn} distances of 2.08-2.26 Å with Mayer bond orders of 0.11-0.23. Similar Ge···H_{Mn} interactions have been observed in some monometallic *cis*-germylene hydride compounds,[42-45,55,56] Additionally, related Si···H interactions were observed in *cis*-$[(dmpe)_2MnH(=SiPh_2)]$ (*cis*-**B** in Scheme 1).[37]

Upon cooling a solution of **6** in d_8-toluene, the Mn*H* ^{1}H NMR signals associated with ***trans*,*trans*-6** and ***cis*,*trans*-6** were unaffected, whereas the Mn*H* signal for ***cis*,*cis*-6** split into four signals (with approximate 2.1 : 1.4 : 1.4 : 1 integration at 209 K), presumably due to slowing of an equilibrium between potential diastereomers (Λ or Δ at each metal centre) and multiple rotamers thereof (*vide infra*). A low rotation barrier for the Mn=Ge bonds in **6** is consistent with the solution behaviour of previously reported manganese germanide complexes.[30] DFT calculations also located three minima of nearly identical (within 1.1 kJ mol^{-1}) energies for ***cis*,*cis*-6** corresponding to the *rac* diastereomer and two rotamers of the *meso* diastereomer, with H–Mn–Mn–H dihedral angles of 84°, 74° and 102°, respectively.

To the best of our knowledge, **6** is only the fourth transition metal μ_2-germanide complex to be crystallographically characterized, and the first to feature hydride co-ligands. While the pathway for the formation of **6** has not been elucidated, this chemistry represents a novel route to a transition metal germanide complex; previous examples were synthesized by acidification of $[Cp^RMn(CO)_2(GeH_3)]^-$ (in one case, acidification of an unidentified intermediate generated by exposure of $[Cp^*Mn(CO)_2(THF)]$ to GeH_4),[30-32] reaction of $[W(CO)_5]^{2-}$ with $[(CO)_5W{=}GeCl_2]$ (1 equiv.) or $GeCl_4$ (0.5 equiv.),[57] or exposure of $GeCl_2$(1,4-dioxane) to 2 equiv. of $[CpRe(nacnac)]^-$ (nacnac = $CH(CMeNAr)_2$; Ar = 2,6-diisopropylphenyl; top of Scheme 3).[34] In fact, the synthesis of complex **6** bears more similarity to that of the cobalt silicide complex $[(\{\kappa^2\text{-}PhB(CH_2P^iPr_2)_2\}CoH_2\{SiH_2R\})(\mu\text{-}Si)(CoH_2\{\kappa^3\text{-}PhB(CH_2P^iPr_2)_3\})]$, which was accessed via the reaction of an anionic cobalt(I) complex with three equivalents of SiH_4 or H_3SiPh in a process which strips silicon of all substituents (bottom of Scheme 3).[36]

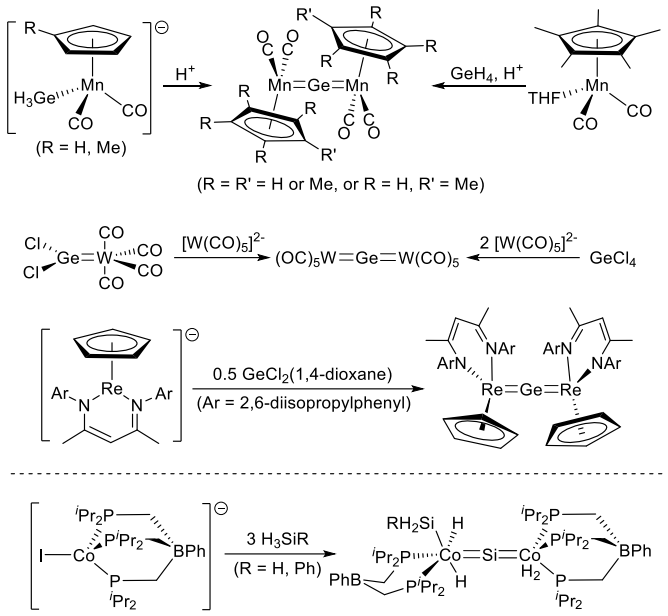

Scheme 3. Top; synthetic routes to previously reported germanide complexes.[30-32] Bottom; synthetic route to a previously reported silicide complex, involving reactivity which strips all substituents from a hydrosilane.[36]

DFT Calculations on the Germylene and Germanide Complexes

DFT calculations were employed to gain insight into the nature of the manganese–germanium bonds in **2a-b**, **3a-b**, and ***trans,trans*-6** (for brevity, referred to in this section as **6**). The geometry optimized (gas phase, all-electron, TZ2P, PBE, ZORA, D3-BJ) structures of **2a**, **3a**, and **6** match well with the X-ray crystal structures (X-ray crystal structures were not obtained for **2b** or **3b**); the Mn–Ge, Mn–P, and (for **2a** and **3a** only) Ge–C bonds are within 0.00-0.03 Å of the crystallographic values, and the Mn–Ge–C angles (for **2a** and **3a**) match within 1.1°.

Multiple bonding character in the germylene and germanide complexes is indicated by large Mn–Ge Mayer bond orders of 1.38-1.44 (cf. ≤0.83 for the Mn–Ge single bonds in **4a-b** and **5a-b**). For the four germylene complexes (Figure 6a and Figure S98), molecular orbitals were located corresponding to localized Mn–Ge σ- and π-bonds. By contrast, Mn–Ge–Mn bonding in **6** (where the Mn–Ge bonds lie in the x-direction) involves four bonding molecular orbitals (Figure 6b); two 3c-2e σ-bonds involving 4s and $4p_x$ orbitals on Ge, and two 3c-2e π-bonds involving the $4p_y$ and $4p_z$ orbitals on Ge (for **6**, the displayed molecular orbitals are from a single point calculation which was carried out using PBE0, to avoid non-intuitive orbital mixing). This results in Mn–Ge bonds with a bond order of two, although each can be considered to be a partial triple bond; *vide supra*. The two 3c-2e π-bonds in **6** contrast the two 2c-2e π-bonds in an allene, and the resulting roughly cylindrical symmetry of the 3-atom π-system explains the low barrier for rotation around the Mn–Ge bonds.[33] This bonding situation is analogous to that described for other transition metal germanide[33] and silicide[35,36] complexes.

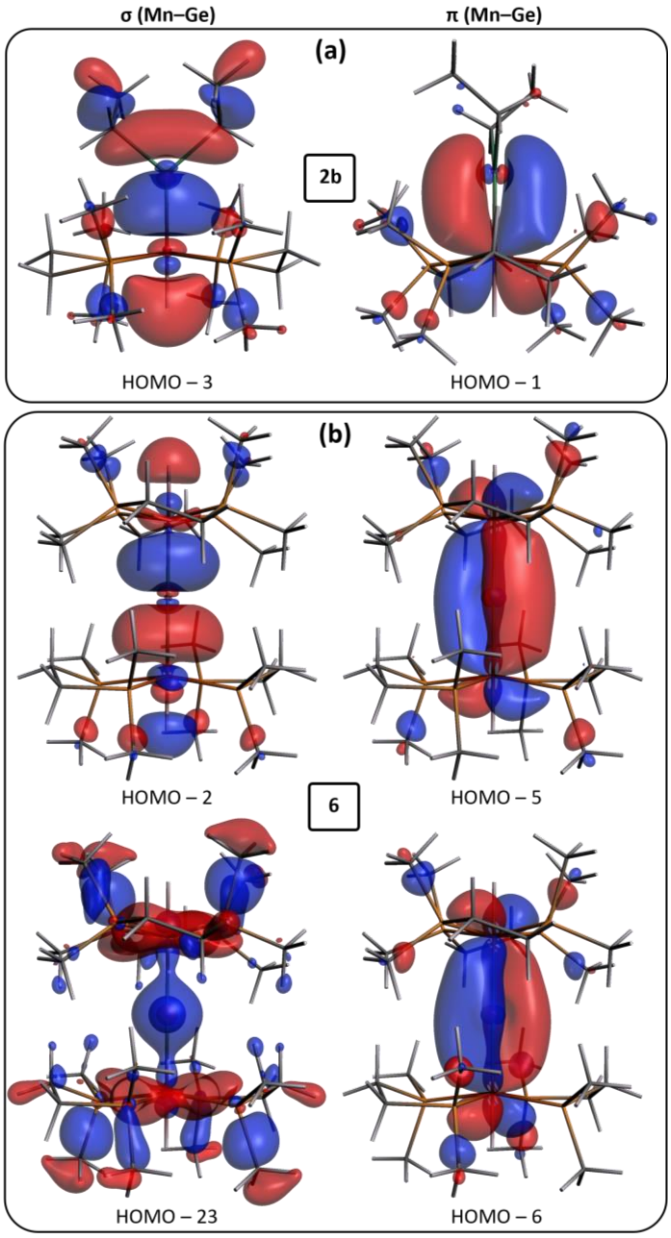

Figure 6. Slater-type σ (left) and π (right) molecular orbitals involved in Mn–Ge bonding in (a) [(dmpe)$_2$MnH(=GeEt$_2$)] (**2b**; qualitatively similar orbitals for **2a**, **3a**, and **3b** are shown in Figure S98) and (b) [{(dmpe)$_2$MnH}$_2$(μ-Ge)] (**6**) with isosurfaces set to 0.03.

Mn–Ge bonding in **2a-b**, **3a-b** and **6** was further investigated via fragment interaction calculations using the energy decomposition analysis (EDA)[58] method of Ziegler and Rauk (Table 1; PBE0, QZ4P, corrected for linear dependency of the wave function). This approach affords an overall interaction energy, ΔE_{int}, which is divided into five components, as shown in Equation 1.[59,60] For **2a-b** and **3a-b** these calculations probed the interaction between a neutral (dmpe)$_2$MnH fragment and a free germylene ligand, whereas for **6**, they considered the interaction between two individual (dmpe)$_2$MnH fragments and a germanium atom (restricted, with a filled 4s-orbital and one filled 4p-orbital). In this analysis, ΔE_{elec} represents the electrostatic interaction energy (calculated using frozen charge distributions for both fragments), ΔE_{Pauli} corresponds to Pauli

repulsion, ΔE_{orb} is the orbital interaction energy (this term includes all contributions resulting from intrafragment polarization), ΔE_{disp} is the dispersion interaction energy, and ΔE_{prep} is the energy needed to bring the fragments from their optimum geometries to their geometries in the unfragmented complex, as well as (for **6**) to bring the germanium atom from its ground-state triplet configuration to the singlet configuration[61] used in the fragment interaction calculation.

$$\Delta E_{int} = \Delta E_{elec} + \Delta E_{Pauli} + \Delta E_{orb} + \Delta E_{disp} + \Delta E_{prep} \qquad (1)$$

The overall interaction energies (ΔE_{int}) for the Mn=Ge double bonds in **2a-b**, **3a-b**, and **6** range from –262 to –267 kJ mol^{-1} (for **6**, the total calculated ΔE_{int} of –526 kJ mol^{-1} corresponds to the delocalized Ge=Mn=Ge system; for all further discussion, the energies of each component of ΔE_{int} in **6** have been divided by 2 to allow for facile comparison to the individual Mn=Ge bonds in **2a-b** and **3a-b**); see Table 1. Notably, significantly stronger electrostatic and orbital contributions were calculated for the germanide complex **6**, though this is offset by somewhat increased Pauli repulsion and a significantly increased preparation energy in **6** (primarily associated with conversion of the Ge atom fragment from a ground-state triplet configuration to the singlet configuration used in the calculation). Hirshfeld charges on the germylene or Ge fragment are –0.26 to –0.32 for **2a-b** and **3a-b**, and –0.55 for **6**.

Table 1. Fragment interaction calculation data for the Mn=Ge bonds in **2a-b** and **3a-b** {(dmpe)$_2$MnH + GeRR'} and **6** {2 × (dmpe)$_2$MnH + a Ge atom with a filled 4s-orbital and one filled 4p-orbital; the resulting energies were divided by two, to afford data equivalent to one Mn=Ge bond}. All energies are in kJ mol^{-1}, ΔE_{int} values are BSSE-corrected, and for ETS-NOCV data, values in parentheses are a percentages of ΔE_{orb}. For **2a-b** and **3a-b**, π1 and π2 are $\pi_{\perp}$ and $\pi_{||}$, respectively. For **6**, σ1 is σ_p and σ2 is σ_s, and $\Delta E_{\pi n}$ includes contributions from a polarization function involving a Ge 5d orbital.

		2a	2b	3a	3b	6
Metal frag(s).		(dmpe)$_2$MnH				
Ligand frag.		GePh$_2$	GeEt$_2$	GeHPh	GeH^{n}Bu	Ge
EDA	ΔE_{elec}	–459	–490	–472	–484	–759
	ΔE_{orb}	–317	–305	–315	–317	–377
	ΔE_{Pauli}	532	558	542	549	795
	ΔE_{Disp}	–53	–40	–34	–31	–51
	ΔE_{prep}	33	8	10	17	129^a
	BSSE	2	1	1	1	1
	ΔE_{int}	–262	–267	–267	–265	–263
ETS-NOCV	$\Delta E_{\sigma 1}$	–122 (39 %)	–134 (44 %)	–129 (41 %)	–135 (43 %)	–137 (36 %)
	$\Delta E_{\sigma 2}$	n/a	n/a	n/a	n/a	–34 (9 %)
	$\Delta E_{\pi 1}$	–128 (40 %)	–117 (38 %)	–125 (40 %)	–127 (40 %)	–99 (26 %)
	$\Delta E_{\pi 2}$	–38 (12 %)	–34 (11 %)	–41 (13 %)	–37 (12 %)	–94 (25 %)
	other	–28 (9 %)	–20 (7 %)	–21 (7 %)	–17 (5 %)	–13 (3 %)

a ΔE_{prep} for **6** is the sum of the energy required to bring the (dmpe)$_2$MnH fragments from their optimum geometries to those in the complex (62 kJ mol^{-1}) and the energy required to bring the Ge atom from its ground-state triplet configuration to the singlet configuration (196 kJ mol^{-1}, experimental).[61] As with other values for **6** in Table 1, ΔE_{prep} has been divided by two to provide energy per Mn=Ge bond.

The deformation density (Δρ) associated with the orbital interaction component (ΔE_{orb}) from fragment interaction calculations on **2a-b**, **3a-b** and **6** was further divided using the Extended Transition State and Natural Orbitals for Chemical Valence (ETS-NOCV) method {Table 1 includes the energies for each component (per Mn=Ge bond)}. Deformation density isosurfaces and the main fragment orbital contributors for **2b** and **6** are shown in Figure 7 (similar figures for **2a** and **3a-b**, and the NOCVs associated with each of the ETS-NOCV contributions, are shown in Figures S100-S104).

For germylene complexes **2a-b** and **3a-b**, two nearly isoenergetic contributions were elucidated; $\Delta\rho_{\sigma}$ involving σ donation from the HOMO of the ligand to the LUMO of the metal fragment, and $\Delta\rho_{\pi(\perp)}$ involving π backdonation from a Mn d orbital (the HOMO of the metal-based fragment) to a vacant p orbital on Ge (the LUMO of the ligand). These contributions are analogous to those for transition metal–carbene bonding.[62] In addition, a weaker third component ($\Delta\rho_{\pi(||)}$) was observed, corresponding to π-backdonation within the plane of the substituents on germanium; the acceptor orbital on the germylene ligand is σ-antibonding with respect to the Ge–R bonds, reminiscent of the acceptor orbitals for a phosphine ligand, which are antibonding with respect to the P–R bonds.[63] A similar bonding description was reported for *trans*-[(dmpe)$_2$MnH(=SiR$_2$)] (**A** and *trans*-**B** in Scheme 1).[37]

The orbital component (ΔE_{orb}) of the Mn=Ge=Mn bonding in [{(dmpe)$_2$MnH}$_2$(μ-Ge)] (**6**) is comprised of two σ donation and two π backdonation interactions, each of which is delocalized over the Mn=Ge=Mn system. The largest contributor ($\Delta\rho_{\sigma(p)}$) involves σ donation from the Ge p_x orbital (the HOMO) to LUMOs of the two Mn-containing fragments. By contrast, the second σ donation interaction ($\Delta\rho_{\sigma(s)}$) involves donation from a Ge s orbital (HOMO-1) to the Mn fragment LUMOs, and is far weaker. The two π backdonation interactions ($\Delta\rho_{\pi(1)}$ and $\Delta\rho_{\pi(2)}$) involve filled Mn d orbitals (HOMO and HOMO-1) and empty Ge p_y and p_z orbitals (LUMO+1 and LUMO, respectively). These interactions are orthogonal and isoenergetic, with interaction energies intermediate between those of $\Delta\rho_{\sigma(p)}$ and $\Delta\rho_{\sigma(s)}$. In addition, the ETS-NOCV calculation identified small contributions (~2% each of the total interaction) from the 5d polarization functions of the Ge basis set, which enhance overlap with Mn pi orbitals (Figure S105).

Summary and Conclusions

Reactions of *trans*-[(dmpe)$_2$MnH(C$_2$H$_4$)] (**1**) with secondary hydrogermanes (H$_2$GeR$_2$) afforded the first base-free terminal germylene complexes of manganese, *trans*-[(dmpe)$_2$MnH(=GeR$_2$)] (R = Ph or Et; **2a-b**). The reaction of **1** with H$_2$GeEt$_2$ mirrors that previously observed with H$_2$SiEt$_2$. By contrast, the previously reported reaction of **1** with H$_2$SiPh$_2$ afforded a mixture of a *trans*-silylene hydride compound (the silicon analogue of **2b**), as well as a *cis*-silylene hydride compound and the silyl dihydride complex [(dmpe)$_2$MnH$_2$(SiHPh$_2$)].[37]

Compounds **2a-b** reacted with primary hydrogermanes (H$_3$GeR') to afford *trans*-[(dmpe)$_2$MnH(=GeHR')] (R' = Ph or ^{n}Bu;

3a-b), which are the only isolated or crystallographically characterized transition metal germylene complexes bearing one H-substituent and one small alkyl or aryl substituent. In the presence of excess primary hydrogermane, **3a-b** exist in equilibrium with the digermyl hydride complexes *mer*-[(dmpe)$_2$MnH(GeH$_2$R')$_2$] (**4a-b**) and the *trans*-hydrogermane germyl complexes *trans*-[(dmpe)$_2$Mn(GeH$_2$R')(HGeH$_2$R')] (**5a-b**). The solution behaviour of **4a-b** differs from that of the silicon analogues, [(dmpe)$_2$MnH(SiH$_2$R')$_2$] (R = Ph or ^{n}Bu; **C** in Scheme 1), which do not exist in equilibrium with a detectable amount of a silyl hydrosilane isomer, and do not eliminate H$_3$SiR' at room temperature to afford a detectable quantity of a silylene hydride complex (although the silylene hydride was observed by high-temperature NMR spectroscopy, and was shown to be accessible through trapping experiments).[38,50]

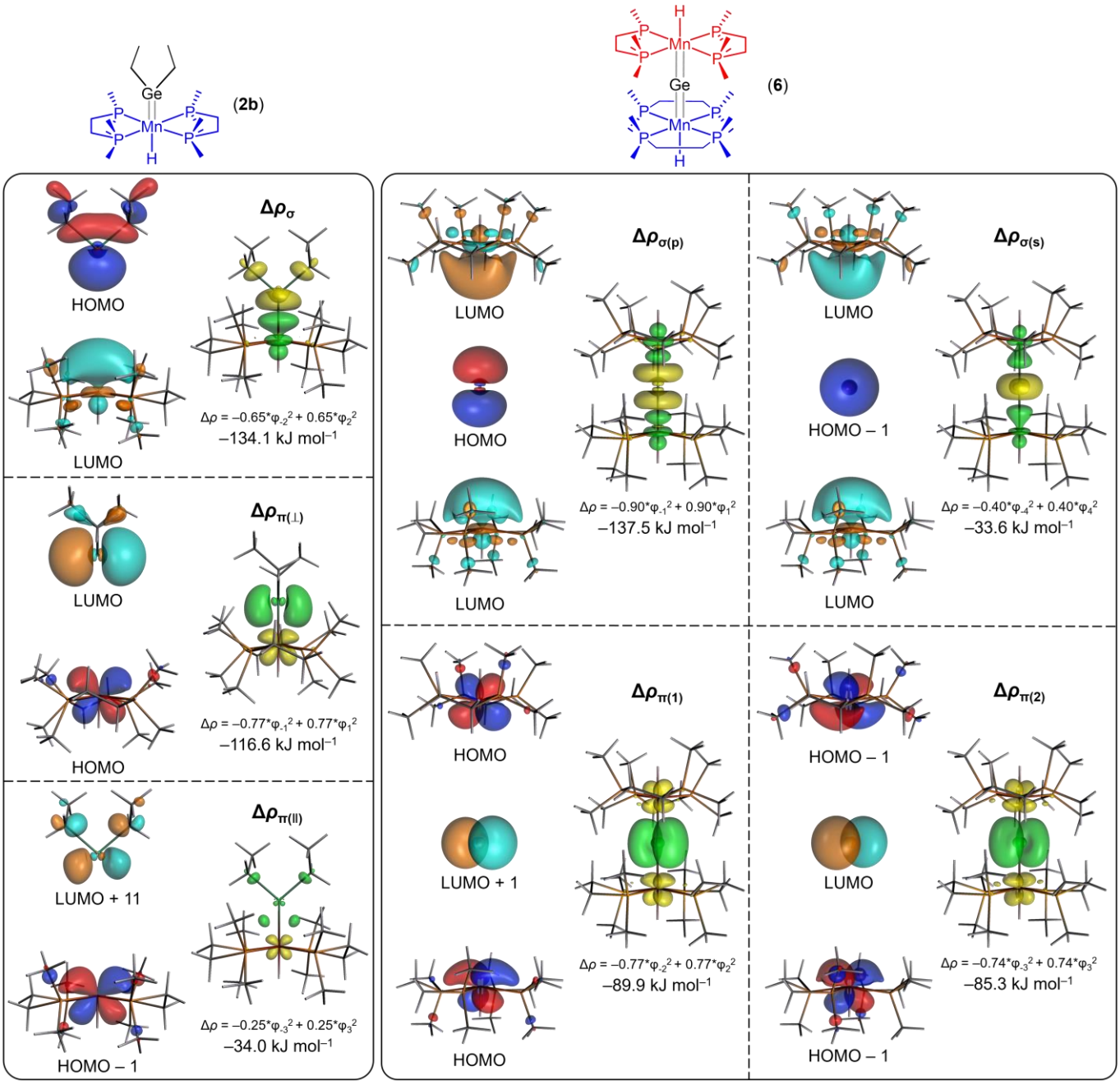

Figure 7. Deformation density contributions and the main fragment orbital contributors to bonding between (left hand side) a (dmpe)$_2$MnH fragment and a GeEt$_2$ fragment in [(dmpe)$_2$MnH(=GeEt$_2$)] (**2b**), and (right hand side) two (dmpe)$_2$MnH fragments and a germanium atom (in a singlet configuration, with one filled 4s and one filled 4p orbital) in [{(dmpe)$_2$MnH}$_2$(μ-Ge)] (**6**). Three major interactions were observed for **2b** ($\Delta\rho_\sigma$, $\Delta\rho_{\pi(\perp)}$, and $\Delta\rho_{\pi(\parallel)}$), and four major interactions were observed for **6** ($\Delta\rho_{\sigma(p)}$, $\Delta\rho_{\sigma(s)}$, $\Delta\rho_{\pi(i)}$, and $\Delta\rho_{\pi(ii)}$). Deformation density isosurfaces (set to 0.0003) are shown in green and yellow, corresponding to increased (green) and decreased (yellow) electron density relative to the non-interacting fragments. Orbital isosurfaces are set to 0.04. Interaction energies for **6** are shown per Mn–Ge bond.

Reactions of **1** with primary hydrogermanes proceeded at elevated temperature to afford mixtures of **3a**-**b**, **4a**-**b** and **5a**-**b**, accompanied by remaining **1**. However, upon continued heating to consume **1**, various unidentified manganese-containing intermediates were formed, ultimately affording the germanide complex [{(dmpe)$_2$MnH}$_2$(μ-Ge)] (**6**) in 30-45% spectroscopic yield. Pure ***trans,trans*-6** was isolated from the reaction of **1** with H_3Ge^nBu, although **6** exists as a mixture of *trans,trans*-, *cis*,*trans*- and *cis,cis*-isomers in solution. The formation of germanide complex **6** is remarkable since it involves stripping of all four substituents from the hydrogermane.

The nature of manganese–germanium bonding in the germylene and germanide complexes was probed through DFT calculations, including fragment interaction calculations with energy decomposition and ETS-NOCV analyses. Nearly identical Mn–Ge bonding energies of –262 to –267 kJ mol^{-1} were determined for the germylene and germanide complexes. For the germylene complexes, ETS-NOCV analysis afforded σ-donation and π-backdonation contributions of similar energy, accompanied by a much weaker π-backdonation interaction where the π bond lies within the MnGeR$_2$ plane. By contrast, the bonding in **6** (starting from two (dmpe)$_2$MnH fragments and a germanium atom with a singlet configuration (one filled 4s orbital and one filled 4p orbital)) is decomposed into four major components, all of which are delocalized over the Mn=Ge=Mn unit: σ donation from a Ge p orbital to the LUMOs of both metal fragments, σ donation from the Ge 4s orbital to the LUMOs of both metal fragments, and two orthogonal and isoenergetic π-backdonation interactions from frontier Mn d orbitals to empty Ge p orbitals (the sum of the energies of the two π components are similar in magnitude of the sum of the energies of the two σ components).

Reactivity of the germylene complexes will be described in a subsequent report.

Experimental

General methods. An argon-filled MBraun UNIlab glove box equipped with a –30 °C freezer was employed for the manipulation and storage of all oxygen- and moisture- sensitive compounds. Air-sensitive preparative reactions were performed on a double-manifold high-vacuum line equipped with a two stage Welch 1402 belt-drive vacuum pump (ultimate pressure 1 × 10^{-4} Torr) using standard techniques.[64] The vacuum was measured periodically using a Kurt J. Lesker 275i convection enhanced Pirani gauge. Residual oxygen and moisture were removed from the argon stream by passage through an Oxisorb-W scrubber from Matheson Gas Products.

Benzene and hexamethyldisiloxane were purchased from Aldrich, hexanes and toluene were purchased from Caledon, and deuterated solvents were purchased from ACP Chemicals. Benzene, C_6D_6, hexamethyldisiloxane, hexanes, toluene, and d_8-toluene were initially dried and distilled at atmospheric pressure from sodium/benzophenone (first four) or sodium (toluene and d_8-toluene). All solvents were stored over an appropriate drying agent (hexamethyldisiloxane, benzene, toluene, d_8-toluene, C_6D_6 = Na/Ph$_2$CO; hexanes = Na/Ph$_2$CO/tetraglyme) and introduced to reactions or solvent storage flasks via vacuum transfer with condensation at –78 °C.

Cl_2GePh_2, Cl_2GeEt_2, 1,4-dioxane, $LiAlH_4$, and ethylmagnesium chloride solution (2.0 M in diethyl ether) were purchased from Sigma-Aldrich. Manganese dichloride was purchased from Strem Chemicals. H_3Ge^nBu and H_3GePh were purchased from Gelest. H_2GePh_2[65] and [(dmpe)$_2$MnH(C$_2$H$_4$)] (**1**)[39,40] were prepared according to literature procedures. H_2GeEt_2 was prepared from a modified version of the H_2GePh_2 procedure as described below. All reagents were used as purchased except (i) H_3GePh and (for some reactions) H_3Ge^nBu, which were purified by vacuum distillation, (ii) 1,4-dioxane, which was dried using sodium/Ph$_2$CO and isolated by vacuum distillation, and (iii) $LiAlH_4$ which was extracted into Et$_2$O, filtered, and isolated by removal of the solvent *in vacuo*. Argon was purchased from PraxAir.

NMR spectroscopy was performed on Bruker AV-500 and AV-600 spectrometers. Spectra were obtained at 298 K unless otherwise indicated. All ^{1}H NMR spectra were referenced relative to SiMe$_4$ through a resonance of the protio impurity of the solvent: C_6D_6 (δ 7.16 ppm) and d_8-toluene (δ 2.08 , 6.97, 7.01, and 7.09 ppm). All ^{13}C NMR spectra were referenced relative to SiMe$_4$ through a resonance of the solvent: C_6D_6 (δ 128.06 ppm) and d_8-toluene (δ 20.43, 125.13, 127.96, 128.87, and 137.48 ppm). The ^{31}P NMR spectra were referenced by indirect referencing from a ^{1}H NMR spectrum.[66] NMR chemical shift abbreviations: s = singlet, d = doublet, t = triplet, q = quartet, quin. = quintet, m = multiplet, app. = apparent, br. = broad. Combustion elemental analyses were performed by the University of Calgary. To allow for easy comparison, selected ^{1}H and ^{31}P NMR data are provided in Table S11.

Single-crystal X-ray crystallographic analyses were performed on crystals coated in Paratone oil and mounted on a a STOE IPDS II diffractometer with an image plate detector in the McMaster Analytical X-Ray (MAX) Diffraction Facility. A semi-empirical absorption correction was applied using redundant and symmetry related data. Raw data was processed using XPREP (as part of the APEX v2.2.0 software), and solved by intrinsic (SHELXT)[67] methods. Structures were completed by difference Fourier synthesis and refined with full-matrix least-squares procedures based on F^2. In all cases, non-hydrogen atoms were refined anisotropically and hydrogen atoms were generated in ideal positions and then updated with each cycle of refinement (with the exception of hydrogen atoms on Mn or Ge, which were located from the difference map and refined isotropically). Refinement was performed with SHELXL[68] in Olex2.[69] To allow for easy comparison (between crystallographic and calculated structures), Mn–Ge, Mn–H and Ge–H bond lengths are listed in Tables S5-7.

2D Powder X-ray diffraction was performed on a Bruker D8 Discover diffractometer equipped with a Vantec 500 area detector and a focused Cu source with Kα radiation (λ = 1.54056 Å) operated at 40 kV and 40 mA. The sample of **6** was packed in a 0.5 mm o.d. special glass (SG; wall thickness 0.01 mm) capillary tube for X-ray diffraction (purchased from Charles Supper Co.) and sealed by inverting to submerge the

open end in a pool of Apiezon H-grease within the glovebox. The powder diffractogram was generated using Gadds and Diffrac.eva. A theoretical diffractogram for ***trans,trans*-6** was generated using Mercury v2020.2.0. Experimental and theoretical diffractograms were viewed using Topas.

All prepared complexes are air sensitive, and their products upon reaction with air are malodorous. Therefore, all syntheses were conducted under an atmosphere of argon.

DFT Calculations. All calculated structures were fully optimized with the ADF/AMS DFT package (SCM, version 2020.102).[70,71] Calculations were conducted in the gas phase within the generalized gradient approximation (GGA) using the 1996 Perdew-Burke-Ernzerhof exchange and correlation functional (PBE),[72] the scalar zeroth-order regular approximation (ZORA)[73-77] for relativistic effects, and Grimme's DFT-D3-BJ dispersion correction.[78,79] Geometry optimizations were conducted using all-electron triple-ζ basis sets with two polarization functions (TZ2P), fine integration grids (Becke[80,81] verygood), and stricter-than-default convergence criteria (gradients = 0.0001, step = 0.002). Calculations were restricted.

Visualization of the computational results was performed using the ADF/AMS-GUI (SCM), Biovia Discovery Studio Visualizer, or the combination of Ortep3 and Pov-Ray v3.7. Orbitals and deformation densities were generated with a fine grid using the densf auxiliary program.

Analytical frequency calculations[82-84] were conducted on all geometry optimized structures (including geometry optimized fragments) to ensure that the geometry optimization led to an energy minimum.

Bond metrics (for all calculations) and Slater-type molecular orbitals (for **2a-b** and **3a-b**) were obtained from the PBE-level calculations described above. However, the molecular orbitals generated from the geometry optimized structure of ***trans,trans*-6** included three of very similar energy which mixed in a non-intuitive manner. By conducting linear combinations of these orbitals, intuitive molecular orbitals were obtained, but could not be assigned as HOMO-*n*. Conducting a single point calculation on this structure using the hybrid PBE0 functional[85,86] (other input keys matched those of the PBE calculations, with the exception of an excellent Becke grid) prevented this unwanted mixing. Therefore, the molecular orbitals shown in Figure 6 for this complex were generated from this calculation, though all bonding metrics discussed were from the PBE-level calculation so they could be directly compared to metrics from the other complexes.

Bonding was analyzed in more detail using a fragment approach (energy decomposition analysis[87,88] with ETS-NOCV analysis[89-92]) that considered the interaction of neutral $(dmpe)_2MnH$ fragments with neutral GeR_2 or Ge ligands. Fragments were generated from the TZ2P geometry optimized structures of each complex, geometries were frozen, and single-point calculations (as well as the EDA/ETS-NOCV calculations) were conducted using the hybrid PBE0 functional[85,86] in conjunction with a quadruple-ζ basis set with four polarization functions (QZ4P), excellent integration grids (Becke[80,81] excellent), and stricter-than-default SCF convergence criteria (1×10^{-7}). The dependency keyword was utilized to prevent issues arising from near-linear dependency of the large function sets. For **6**, two $(dmpe)_2MnH$ fragments and a single Ge fragment were employed, and integer orbital occupations was enforced for the Ge fragment using the key 'OCCUPATIONS IntegerAufbou' (this was done to avoid non-integer 4p orbital occupations). Preparation energies (ΔE_{prep}) were obtained for nearly all fragments by allowing the fragments to adopt equilibrium geometries (using the same method previously described for geometry optimization, though energies were obtained by single point calculations using the parameters described above for other single point calculations), while for the Ge fragment in **6** this was obtained by consulting the NIST Atomic Spectra Database version 5.10.[61] Basis set superposition errors (BSSEs) were calculated through the use of ghost atoms with no nuclear charge and no electrons to contribute to the molecule (using the molecular fragments method).

H_2GeEt_2. 0.606 g (18.3 mmol) of $LiAlH_4$ was added to 20 mL of tetraglyme, and the suspension was stirred for 2 hours to ensure complete dissolution of the solid. 2.180 g (10.8 mmol) of Cl_2GeEt_2 dissolved in 5 mL of tetraglyme was added slowly to the reaction mixture, resulting in precipitation of white solid which dissolved immediately after addition was complete. The clear, colourless solution was stirred at room temperature for 2 days, at which point it was freeze/pump/thawed three times. H_2GeEt_2 (0.912 g, 6.9 mmol, 64 %) was isolated as a clear, colourless liquid by room temperature distillation to a collection flask cooled to –78 °C. **^{1}H NMR (C_6D_6, 600 MHz, 298 K):** δ 3.85 (quin., 2H, $^3J_{H,H}$ 3.2 Hz, Ge*H*), 1.03 (t, 6H, $^3J_{H,H}$ 7.9 Hz, CH_2CH_3), 0.78 (m, 4H, CH_2CH_3).

$[(dmpe)_2MnH(=GePh_2)]$ (2a). 275.1 mg (0.72 mmol) of $[(dmpe)_2MnH(ethylene)]$ (**1**) was dissolved in 10 mL of benzene and placed in a 100 mL storage flask. To this yellow solution was added 408.9 mg (1.79 mmol) of H_2GePh_2, at which point the flask was sealed and heated at 55 °C with stirring for 5 days in the dark to afford a dark orange solution. The solvent was then removed *in vacuo*, and the resulting solid was washed with 10 mL of hexanes (to remove excess H_2GePh_2) followed by recrystallization from toluene layered with hexanes (at –30 °C) to yield 264.7 mg (0.45 mmol) of **2a** as very dark red crystals. The mother liquors were evaporated to dryness *in vacuo*, and resulting solid was again recrystallized from toluene layered with hexanes (at –30 °C) to afford an additional 65.8 mg (0.11 mmol) of **2a**, for a combined yield of 78 %. X-ray quality crystals were obtained from a dilute solution of **2a** in hexanes at –30 °C. **^{1}H NMR (C_6D_6, 600 MHz, 298 K):** δ 7.61 (d of d, 4H, $^3J_{H,H}$ 7.6 Hz, $^4J_{H,H}$ 1.2 Hz, *o*-C*H*), 7.25 (t, 4H, $^3J_{H,H}$ 7.6 Hz, *m*-C*H*), 7.11 (t of t, 2H, $^3J_{H,H}$ 7.4 Hz, $^4J_{H,H}$ 1.4 Hz, *p*-C*H*), 1.99, 1.70 (2 × m, 4H, PCH_2), 1.38, 1.14 (2 × s, 12H, PCH_3), –10.02 (quin., 1H, $^2J_{H,P}$ 55.7 Hz, Mn*H*). **^{13}C{^{1}H} NMR (C_6D_6, 151 MHz, 298 K):** δ 168.88 (s, *i*-*C*), 132.46 (s, *o*-*C*H), 127.67 (s, *m*-*C*H), 126.47 (s, *p*-*C*H), 34.25 (m, PCH_2), 29.10 (m, PCH_3). **^{31}P{^{1}H} NMR (C_6D_6, 243 MHz, 298 K):** δ 79.67 (s). **Anal.** found (calcd): C, 49.29 (49.44); H, 7.57 (7.43).

[(dmpe)$_2$MnH(=GeEt$_2$)] (2b). 364.1 mg (0.95 mmol) of [(dmpe)$_2$MnH(C$_2$H$_4$)] (1) was dissolved in 30 mL of benzene and placed in a 100 mL storage flask. To this yellow solution was added 405 mg (3.05 mmol) of H$_2$GeEt$_2$, at which point the reaction vessel was sealed and covered in aluminium foil. Stirring at 60 °C for three days in the dark afforded a very dark orange solution, and removal of the solvent and excess hydrogermane *in vacuo* yielded a yellow-brown powder. Recrystallization from a concentrated hexanes solution at –30 °C afforded 197.2 mg (0.40 mmol) of dark brown/black crystals. Concentrating the mother liquor and allowing it to stand at –30 °C afforded an additional 122.6 mg (0.25 mmol), for a combined yield of 0.65 mmol (68 %). **^{1}H NMR (C$_6$D$_6$, 600 MHz, 298 K):** δ 1.87, 1.74 (2 × m, 4H, PC*H*$_2$), 1.51 (q, 4H, $^3J_{H,H}$ 7.9 Hz, C*H*$_2$CH$_3$), 1.32, 1.20 (2 × s, 12H, PC*H*$_3$), 1.30 (t, 6H, $^3J_{H,H}$ 8.0 Hz, CH$_2$C*H*$_3$), –10.79 (quin., 1H, $^2J_{H,P}$ 52.1 Hz, Mn*H*). **^{13}C{^{1}H} NMR (C$_6$D$_6$, 151 MHz, 298 K):** δ 35.54 (s, *C*H$_2$CH$_3$), 34.68 (m, P*C*H$_2$), 30.08, 28.90 (2 × m, P*C*H$_3$), 9.56 (s, CH$_2$*C*H$_3$). **^{31}P{^{1}H} NMR (C$_6$D$_6$, 243 MHz, 298 K):** δ 79.90 (s). **Anal.** found (calcd): C, 39.35 (39.46); H, 8.94 (8.90).

[(dmpe)$_2$MnH(=GeHPh)] (3a). 7.9 mg (0.02 mmol) of [(dmpe)$_2$MnH(=GeEt$_2$)] (**2b**) was dissolved in approximately 0.7 mL of C$_6$D$_6$, and to the resulting clear bronze solution was added 9.9 mg (0.06 mmol) of H$_3$GePh. After allowing the reaction mixture to sit at room temperature for 1.5 h (with no significant visible change), the solvent and free hydrogermanes were removed *in vacuo* and the and the resulting red oil was left under dynamic vacuum (~10 mTorr) for 1.5 h. The residue was then re-dissolved in C$_6$D$_6$, volatiles were again removed *in vacuo*, and resulting oil was left under dynamic vacuum (~10 mTorr) for 1 h. Dissolving this oil in C$_6$D$_6$ afforded a clear red solution which was analysed by NMR spectroscopy. Within 15 minutes of dissolution, the dominant species in solution was **3a**, though 7 hydride-containing decomposition products were also observed (the most intense Mn*H* signal in the ^{1}H NMR spectrum was 12% of the intensity of the Mn*H* signal for **3a**), and the concentrations of these decomposition products increased dramatically over time (the cumulative intensity of the Mn*H* ^{1}H NMR signals relative to the Mn*H* environment of **3a** was 41% overnight at room temperature, increasing to 56% after 2 days). Given the instability of **3a**, it was not isolated with analytical purity. X-ray quality crystals of **3a** were obtained by repeating the reaction of **2b** (26.8 mg) with H$_3$GePh (34.7 mg) in 3 mL of benzene, removing volatiles *in vacuo* to afford an oil, allowing it to sit for two hours at room temperature *in vacuo*, and crystallization from toluene layered with hexanes at –30 °C. **^{1}H NMR (C$_6$D$_6$, 500 MHz, 298 K):** δ 12.68 (m, 1H, Ge*H*), 8.21 (d, 2H, $^3J_{H,H}$ 7.4 Hz, *o*-C*H*), 7.38 (t, 2H, $^3J_{H,H}$ 7.4 Hz, *m*-C*H*), 7.19 (t, 1H, $^3J_{H,H}$ 7.5 Hz, *p*-C*H*), 2.12, 1.78 (2 × m, 4H, PC*H*$_2$), 1.31, 1.14 (2 × s, 12H, PC*H*$_3$), –9.18 (quin., 1H, $^2J_{H,P}$ 54.2 Hz, Mn*H*). **^{13}C{^{1}H} NMR (C$_6$D$_6$, 126 MHz, 298 K):** δ 164.04 (s, *i*-*C*), 135.12 (s, *o*-*C*H), 128.26 (*m*-*C*H),‡‡ 126.99 (s, *p*-*C*H), 34.22 (app. quin., $J_{C,P}$ 12.1 Hz, P*C*H$_2$), 28.82, 28.07 (2 × m, P*C*H$_3$). **^{31}P{^{1}H} NMR (C$_6$D$_6$, 202 MHz, 298 K):** δ 78.64 (s).

[(dmpe)$_2$MnH(=GeH^{n}Bu)] (3b). 207 mg (0.43 mmol) of [(dmpe)$_2$MnH(=GeEt$_2$)] (**2b**) was dissolved in 15 mL of benzene and placed in a 50 mL storage flask. To this solution was added 323 mg (2.43 mmol) of H$_3$Ge^{n}Bu. The reaction vessel was sealed, and the solution was stirred in the dark for 2 hours at room temperature, at which point volatiles (solvent and free hydrogermanes) were removed *in vacuo*, and the residue was left under dynamic vacuum for 2 hours (also in the dark). This bronze oil was dissolved in 10 mL of toluene and volatiles were removed *in vacuo*. This dissolution/evacuation procedure was repeated, and the resulting oil was recrystallized from hexamethyldisiloxane at –30 °C to afford 114.5 mg of **3b** as a brown powder. Concentrating the mother liquor and letting it stand at –30 °C yielded an additional 26.9 mg of **3b**, for a combined yield of 0.29 mmol (68 %). **^{1}H NMR (C$_6$D$_6$, 500 MHz, 298 K): δ** 12.38 (m, 1H, Ge*H*), 2.04 (quin., 2H, $^3J_{H,H}$ 7.6 Hz, CH$_2$C*H*$_2$CH$_2$CH$_3$), 1.86, 1.71 (2 × m, 4H, PC*H*$_2$), 1.63 (m, 2H, C*H*$_2$CH$_2$CH$_2$CH$_3$), 1.52 (sextet, 2H, $^3J_{H,H}$ 7.4 Hz, CH$_2$CH$_2$C*H*$_2$CH$_3$), 1.36, 1.18 (2 × s, 12H, PC*H*$_3$), 1.02 (t, 3H, $^3J_{H,H}$ 7.3 Hz, CH$_2$CH$_2$CH$_2$C*H*$_3$), –9.82 (quin., 1H, $^2J_{H,P}$ 52.5 Hz, Mn*H*). **^{1}H NMR (*d*$_8$-toluene, 500 MHz, 298 K): δ** 12.26 (m, 1H, Ge*H*), 1.96 (quin. of m, 2H, $^3J_{H,H}$ 7.6 Hz, CH$_2$C*H*$_2$CH$_2$CH$_3$), 1.82, 1.68 (2 × m, 4H, PC*H*$_2$), 1.55 (m, 2H, C*H*$_2$CH$_2$CH$_2$CH$_3$), 1.47 (sextet, 2H, $^3J_{H,H}$ 7.4 Hz, CH$_2$CH$_2$C*H*$_2$CH$_3$), 1.33, 1.15 (2 × s, 12H, PC*H*$_3$), 0.99 (t, 3H, $^3J_{H,H}$ 7.4 Hz, CH$_2$CH$_2$CH$_2$C*H*$_3$), –9.91 (quin., 1H, $^2J_{H,P}$ 52.6 Hz, Mn*H*). **^{13}C{^{1}H} NMR (C$_6$D$_6$, 126 MHz, 298 K):** δ 46.35 (s, *C*H$_2$CH$_2$CH$_2$CH$_3$), 34.27 (app. quin., $J_{C,P}$ 12.2 Hz, P*C*H$_2$), 32.68 (s, CH$_2$*C*H$_2$CH$_2$CH$_3$), 28.95, 28.22 (2 × m, P*C*H$_3$), 26.93 (s, CH$_2$CH$_2$*C*H$_2$CH$_3$), 14.51 (s, CH$_2$CH$_2$CH$_2$*C*H$_3$). **^{31}P{^{1}H} NMR (C$_6$D$_6$, 202 MHz, 298 K):** δ 78.55 (s). **^{31}P{^{1}H} NMR (*d*$_8$-toluene, 202 MHz, 298 K):** δ 78.55 (s). **Anal.** found (calcd): C, 39.17 (39.46); H, 8.56 (8.90).

Mixture of [(dmpe)$_2$MnH(=GeHPh)] (3a), *mer*-[(dmpe)$_2$MnH(GeH$_2$Ph)$_2$] (4a) and *trans*-[(dmpe)$_2$Mn(GeH$_2$Ph)(HGeH$_2$Ph)] (5a). (method a) 13.4 mg (0.02 mmol) of [(dmpe)$_2$MnH(=GePh$_2$)] (**2a**) and 18.0 mg (0.12 mmol) of H$_3$GePh were dissolved in approximately 0.7 mL of C$_6$D$_6$ and sealed in a J-young NMR tube. The reaction mixture was allowed to sit at room temperature for 1.5 hours, at which point the solution was analyzed by NMR spectroscopy, revealing a 5 : 2 : 1 ratio of **3a** : **4a** : **4a** (no **2a** was detected spectroscopically). (method b) method a was repeated using 12.7 mg (0.03 mmol) of [(dmpe)$_2$MnH(=GeEt$_2$)] (**2b**) and 15.9 mg (0.10 mmol) of H$_3$GePh. After ~24 hours, the solution was analyzed by NMR spectroscopy, revealing a 1 : 125 : 56 : 26 ratio of **2b** : **3a** : **4a** : **5a**. (method c) method a was repeated using 12.0 mg (0.02 mmol) of [(dmpe)$_2$MnH(=GeEt$_2$)] (**2b**) and 15.0 mg (0.10 mmol), as well as *d*$_8$-toluene in place of C$_6$D$_6$. After 80 minutes, the solution was analyzed by NMR spectroscopy, revealing a 6 : 2 : 1 ratio of **3a** : **4a** : **5a** (no **2b** was detected spectroscopically). **4a**: **^{1}H NMR (C$_6$D$_6$, 500 MHz, 298 K):** δ 8.00 (d of d, 4H, $^3J_{H,H}$ 7.8 Hz, $^4J_{H,H}$ 1.1 Hz, *o*-C*H*), 7.27 (t, 4H, $^3J_{H,H}$ 7.2 Hz, *m*-C*H*), 7.21 (t, 2H, $^3J_{H,H}$ 7.4 Hz, *p*-C*H*),‡‡ 4.94, 4.93 (2 × m, 2H, Ge*H*),‡‡ 1.45 (d, 6H, $^2J_{H,P}$ 5.4 Hz, PC*H*$_3$), 1.39, 1.22, 1.08, 0.90 (4 × m, 2H, PC*H*$_2$), 1.20 (d, 6H, $^2J_{H,P}$ 6.7 Hz, PC*H*$_3$), 0.99 (d, 6H, $^2J_{H,P}$ 5.9 Hz, PC*H*$_3$), 0.88 (d, 6H, $^2J_{H,P}$ 4.0 Hz, PC*H*$_3$), –11.37 (quin.,

1H, $^2J_{H,P}$ 22.7 Hz, Mn*H*). **^{13}C{^{1}H} NMR (C_6D_6, 126 MHz, 298 K):** δ 148.82 (s, *i*-*C*), 136.82 (s, *o*-*C*H), 127.63 (s, *m*-*C*H), 33.12, 31.52 (2 × m, P*C*H$_2$), 23.51 (t, $J_{C,P}$ 6.4 Hz, P*C*H$_3$), 22.19 (d, $J_{C,P}$ 14.5 Hz, P*C*H$_3$), 21.88 (d, $J_{C,P}$ 16.4 Hz, P*C*H$_3$), 18.47 (d, $J_{C,P}$ 25.2 Hz, P*C*H$_3$). **^{31}P{^{1}H} NMR (C_6D_6, 202 MHz, 298 K):** δ 67.89, 62.05 (2 × s, 2P). **^{1}H NMR (d_8-toluene, 500 MHz, 198 K):** δ 8.13 (d, 4H, $^3J_{H,H}$ 7.0 Hz, *o*-C*H*), 7.33 (t, 4H, $^3J_{H,H}$ 7.2 Hz, *m*-C*H*), 7.25 (t, 2H, $^3J_{H,H}$ 7.6 Hz, *p*-C*H*), 5.00, 4.88 (2 × s, 2H, Ge*H*),[§§] 1.40, 0.73 (2 × s, 6H, PC*H*$_3$), 1.24, 1.10, 0.96, 0.71 (4 × m, 2H, PC*H*$_2$), 1.10 (d, 6H, $^2J_{H,P}$ 6.5 Hz, PC*H*$_3$), 0.87 (d, 6H, $^2J_{H,P}$ 5.3 Hz, PC*H*$_3$), –11.78 (quin., 1H, $^2J_{H,P}$ 25.3 Hz, Mn*H*). **^{13}C{^{1}H} NMR (d_8-toluene, 126 MHz, 198 K):** δ 149.07 (s, *i*-*C*), 136.59 (s, *o*-*C*H), 127.51 (s, *m*-*C*H), 126.75 (s, *p*-*C*H), 32.31, 30.43 (2 × m, P*C*H$_2$), 22.37 (t, $J_{C,P}$ 6.1 Hz, P*C*H$_3$), 21.94 (m, 2 × P*C*H$_3$), 17.08 (d, $J_{C,P}$ 24.0 Hz, P*C*H$_3$). **^{31}P{^{1}H} NMR (d_8-toluene, 202 MHz, 198 K):** δ 68.56, 63.07 (2 × t, $^2J_{P,P}$ 33.5 Hz, 2P). **5a**: **^{1}H NMR (C_6D_6, 500 MHz, 298 K):** δ 7.82 (d of d, 4H, $^3J_{H,H}$ 7.9 Hz, $^4J_{H,H}$ 1.2 Hz, *o*-C*H*), 7.22 (t, 4H, $^3J_{H,H}$ 7.0 Hz, *m*-C*H*),[‡‡] 7.17 (t, 2H, $^3J_{H,H}$ 7.4 Hz, *p*-C*H*),[‡‡] 4.72 (m, 4H, terminal Ge*H*), 1.51 (d, 8H, $^2J_{H,P}$ 9.9 Hz, PC*H*$_2$), 1.28 (s, 24H, PC*H*$_3$), –11.96 (quin., 1H, $^2J_{H,P}$ 33.3 Hz, Ge*H*Mn). **^{13}C{^{1}H} NMR (C_6D_6, 126 MHz, 298 K):** δ 136.46 (s, *o*-*C*H), 31.52 (m, P*C*H$_2$), 22.45 (m, P*C*H$_3$). **^{31}P{^{1}H} NMR (C_6D_6, 202 MHz, 298 K):** δ 64.93 (s). **^{1}H NMR (d_8-toluene, 500 MHz, 198 K):** δ 7.84 (d, 4H, $^3J_{H,H}$ 7.0 Hz, *o*-C*H*), 7.22 (m, *m*-C*H* and *p*-C*H*),[‡‡] 5.13 (s, 2H, terminal Ge$H_{hydrogermane}$),[§] 4.31 (s, 2H, terminal GeH_{germyl}),[§] –12.03 (quin., 1H, $^2J_{H,P}$ 33.7 Hz, Ge*H*Mn). **^{31}P{^{1}H} NMR (d_8-toluene, 202 MHz, 198 K):** δ 66.42 (s). **Signals not definitively assigned to 4b or 5b: ^{13}C{^{1}H} NMR (C_6D_6, 126 MHz, 298 K):** δ 126.86, 126.75 (2 × s). **^{13}C{^{1}H} NMR (d_8-toluene, 126 MHz, 198 K):** δ 32.30, 23.36, 14.69 (3 × s).

Mixture of [(dmpe)$_2$MnH(=GeH^{n}Bu)] (3b), *mer*-[(dmpe)$_2$MnH(GeH$_2$^{n}Bu)$_2$] (4b) and *trans*-[(dmpe)$_2$Mn(GeH$_2$^{n}Bu)(HGeH$_2$^{n}Bu)] (5b). (method a) 11.4 mg (0.02 mmol) of [(dmpe)$_2$MnH(=GePh$_2$)] (**2a**) and 5.2 mg (0.04 mmol) of H$_3$Ge^{n}Bu were dissolved in approximately 0.7 mL of C_6D_6 and sealed in a J-young NMR tube. The reaction mixture was allowed to sit at room temperature overnight, and then the solution was analyzed by NMR spectroscopy, revealing a 1 : 19 : 17 : 5 ratio of **2a** : **3b** : **4b** : **5b**. (method b) method a was repeated using 16.2 mg (0.03 mmol) of [(dmpe)$_2$MnH(=GeEt$_2$)] (**2b**) and 17.7 mg (0.13 mmol) of H$_3$Ge^{n}Bu. After 1 hour, the solution was analyzed by NMR spectroscopy, revealing a 3 : 4 : 1 ratio of **3b** : **4b** : **5b** (no **2b** was detected spectroscopically). (method c) method a was repeated using 14.6 mg (0.03 mmol) of [(dmpe)$_2$MnH(=GeH^{n}Bu)] (**3b**) and 16.0 mg (0.12 mmol) of H$_3$Ge^{n}Bu in approximately 0.7 mL of d_8-toluene. The reaction mixture was allowed to sit at room temperature overnight, and the solution was then analyzed by NMR spectroscopy, revealing a 5 : 4 : 1 ratio of **3b** : **4b** : **5b**. **4b: ^{1}H NMR (d_8-toluene, 600 MHz, 298 K):** δ 4.09 (s, 2H, Ge*H*), 3.87 (m, 2H, Ge*H*), 1.90 (quin., 4H, $^3J_{H,H}$ 7.6 Hz, CH$_2$C*H*$_2$CH$_2$CH$_3$), 1.60 (sextet, 4H, $^3J_{H,H}$ 7.4 Hz, CH$_2$CH$_2$C*H*$_2$CH$_3$), 1.46, 1.23 (2 × PC*H*$_2$),[‡‡] 1.37 (d, 6H, $^2J_{H,P}$ 4.7 Hz, PC*H*$_3$), 1.28 (quin., 4H, $^3J_{H,H}$ 7.0 Hz, C*H*$_2$CH$_2$CH$_2$CH$_3$),[‡‡] 1.24 (d, 6H, $^2J_{H,P}$ 5.5 Hz, PC*H*$_3$), 1.04 (t, 6H, $^3J_{H,H}$ 7.4 Hz, CH$_2$CH$_2$CH$_2$C*H*$_3$), 1.01 (d, 6H, $^2J_{H,P}$ 5.0 Hz, PC*H*$_3$), 0.98 (m, 6H, PC*H*$_3$), 0.87 (m, 2H, PC*H*$_2$), –10.41 (t., 1H, $^2J_{H,P}$ 19.8 Hz, Mn*H*). **^{13}C{^{1}H} NMR (d_8-toluene, 151 MHz, 298 K):** δ 35.74 (s, CH$_2$*C*H$_2$CH$_2$CH$_3$), 34.12, 31.34, 29.73 (3 × m, P*C*H$_2$), 27.04 (s, CH$_2$CH$_2$*C*H$_2$CH$_3$), 23.82 (t, $J_{C,P}$ 6.0 Hz, P*C*H$_3$), 21.12 (s, *C*H$_2$CH$_2$CH$_2$CH$_3$), 20.34 (P*C*H$_3$),[‡‡] 19.82, 18.18 (2 × m, P*C*H$_3$), 14.39 (s, CH$_2$CH$_2$CH$_2$*C*H$_3$). **^{31}P{^{1}H} NMR (d_8-toluene, 243 MHz, 298 K):** δ 71.88 (s, 2P), 59.44 (s, 2P). **^{1}H NMR (d_8-toluene, 600 MHz, 222 K):** δ 4.25 (s, 2H, Ge*H*), 3.98 (m, 2H, $J_{H,H}$ 6.6 Hz,[‡‡] Ge*H*), 2.03 (quin., 4H, $^3J_{H,H}$ 7.8 Hz, CH$_2$C*H*$_2$CH$_2$CH$_3$), 1.68 (sextet, 4H, $^3J_{H,H}$ 7.4 Hz, CH$_2$CH$_2$C*H*$_2$CH$_3$), 1.40 (PC*H*$_2$),[‡‡] 1.39 (m, 4H, C*H*$_2$CH$_2$CH$_2$CH$_3$), 1.37, 0.89 (2 × s, 6H, PC*H*$_3$), 1.25 (d, 6H, $^3J_{H,H}$ 5.0 Hz, PC*H*$_3$), 1.20, 0.70 (2 × PC*H*$_2$),[‡‡] 1.11 (t, 6H, $^3J_{H,H}$ 7.3 Hz, CH$_2$CH$_2$CH$_2$C*H*$_3$), 0.94 (d, 6H, $^3J_{H,H}$ 4.7 Hz, PC*H*$_3$), –10.16 (t, 1H, $^2J_{H,P}$ 18.7 Hz, Mn*H*). **^{13}C{^{1}H} NMR (d_8-toluene, 126 MHz, 222 K):** δ 36.18 (s, CH$_2$*C*H$_2$CH$_2$CH$_3$), 33.73, 28.27 (2 × m, P*C*H$_2$), 27.45 (s, CH$_2$CH$_2$*C*H$_2$CH$_3$), 22.72 (t, $J_{C,P}$ 6.1 Hz, P*C*H$_3$), 22.00 (s, *C*H$_2$CH$_2$CH$_2$CH$_3$), 19.37 (m, P*C*H$_3$), 19.09 (d of d, $J_{C,P}$ 9.2 Hz, 4.2 Hz, P*C*H$_3$), 16.84 (t, $J_{C,P}$ 15.2 Hz, P*C*H$_3$), 14.65 (s, CH$_2$CH$_2$CH$_2$*C*H$_3$). **^{31}P{^{1}H} NMR (d_8-toluene, 202 MHz, 222 K):** δ 73.21, 58.79 (2 × t, 2P, $^2J_{P,P}$ 25.3 Hz). **5b**: **^{1}H NMR (d_8-toluene, 600 MHz, 298 K):** δ 3.71 (br. s, 4H, terminal Ge*H*), 1.81 (quin., 4H, $^3J_{H,H}$ 7.7 Hz, CH$_2$C*H*$_2$CH$_2$CH$_3$),[‡‡] 1.53 (sextet, 4H, $^3J_{H,H}$ 7.4 Hz, CH$_2$CH$_2$C*H*$_2$CH$_3$),[‡‡] 1.30 (m, 24H, PC*H*$_3$), 1.01 (t, 6H, $^3J_{H,H}$ 7.6 Hz, CH$_2$CH$_2$CH$_2$C*H*$_3$), 0.88 (m, 4H, C*H*$_2$CH$_2$CH$_2$CH$_3$), –12.01 (quin., 1H, $^2J_{H,P}$ 31.7 Hz, Ge*H*Mn). **^{13}C{^{1}H} NMR (d_8-toluene, 151 MHz, 298 K):** δ 35.74 (s, CH$_2$*C*H$_2$CH$_2$CH$_3$), 27.12 (s, CH$_2$CH$_2$*C*H$_2$CH$_3$), 22.52 (br. s, P*C*H$_3$), 21.84 (s, *C*H$_2$CH$_2$CH$_2$CH$_3$), 14.39 (s, CH$_2$CH$_2$CH$_2$*C*H$_3$). **^{31}P{^{1}H} NMR (d_8-toluene, 243 MHz, 298 K):** δ 68.03 (s). **^{1}H NMR (d_8-toluene, 600 MHz, 222 K):** δ 4.29 (s, 2H, terminal Ge$H_{hydrogermane}$),[‡‡] 3.29 (s, 2H, terminal GeH_{germyl}), 1.34 (s, 12H, PC*H*$_3$), 1.20 (PC*H*$_3$),[‡‡] –11.90 (quin., 1H, $^2J_{H,P}$ 31.7 Hz, Ge*H*Mn). **^{31}P{^{1}H} NMR (d_8-toluene, 202 MHz, 222 K):** δ 68.95 (s). **Signals not definitively assigned to 4b or 5b; ^{13}C{^{1}H} NMR (d_8-toluene, 151 MHz, 222 K):** δ 30.43, 23.70 (2 × m).

[{(dmpe)$_2$MnH}$_2$(μ-Ge)] (6). (method a) 255.6 mg (0.66 mmol) of [(dmpe)$_2$MnH(C$_2$H$_4$)] (**1**) was dissolved in 20 mL of benzene and placed in a 50 mL storage flask. To this yellow solution was added 354.3 mg (2.67 mmol) of H$_3$Ge^{n}Bu. After sealing the flask, the solution was heated in the dark for 2 days at 80 °C, then 2 more days at 100 °C to afford a dark red solution. After removing the volatiles *in vacuo*, the resulting oil was washed with 2 mL of hexanes and then dissolved in 5 mL of toluene. This solution was centrifuged to remove insoluble material and cooled to –30 °C to afford 72.5 mg (0.09 mmol, 27 %) of **6** as very large dark red (almost black) crystals with analytical purity. (method b) 187.9 mg (0.49 mmol) of [(dmpe)$_2$MnH(C$_2$H$_4$)] (**1**) and 165 mg (1.08 mmol) of H$_3$GePh were dissolved in 20 mL of benzene and placed in a 50 mL storage flask. This solution was stirred for two days in the dark at 80 °C, and the volatiles were removed *in vacuo*. The residue was dissolved in hexanes, centrifuged to remove insoluble material, and kept at –30 °C for a week to afford 12.7 mg (0.02 mmol, 7 %) of **6** as red crystals which were of X-ray quality and pure by NMR spectroscopy. Attempts to increase this yield by recrystallization (from toluene) of the material which didn't dissolve in hexanes afforded impure product. (method c) 12.8 mg (0.03 mmol) of [(dmpe)$_2$MnH(C$_2$H$_4$)] (**1**), 10.2 mg (0.07 mmol) of H$_3$GePh, and 8.2 mg (0.03 mmol) of hexaethylbenzene internal standard were dissolved in approximately 0.7 mL of C_6D_6 and sealed in a

J-young NMR tube. The reaction mixture was heated at 80 °C, and periodically monitored spectroscopically. After 5 days at this temperature, 49% conversion to **6** was observed, accompanied by a variety of unidentified species. (method d) 14.2 mg (0.04 mmol) of [(dmpe)$_2$MnH(C$_2$H$_4$)] (**1**), 9.8 mg (0.07 mmol) of H$_3$Ge^{n}Bu, and 9.1 mg (0.04 mmol) of hexaethylbenzene internal standard were dissolved in approximately 0.7 mL of C$_6$D$_6$ and sealed in a J-young NMR tube. The reaction mixture was heated at 80 °C, and periodically monitored spectroscopically. After 5 days at this temperature, 17% conversion to **6** was observed, accompanied by a variety of unidentified species. Ratio of ***trans*,*trans*-6** : ***cis*,*cis*-6** : ***cis*,*trans*-6** is 11 : 5 : 1 (298 K), 8 : 6 : 1 (334 K), 15 : 6 : 1 (189 K) by NMR spectroscopy. ***trans*,*trans*-6: ^{1}H NMR (C$_6$D$_6$, 600 MHz, 298 K):** δ 1.97, 1.13 (2 × s, 24H, PC*H*$_3$), 1.92, 1.72 (2 × m, 8H, PC*H*$_2$), –22.67 (quin., $^2J_{H,P}$ 52.4 Hz, 2H, Mn*H*). **^{13}C{^{1}H} NMR (C$_6$D$_6$, 151 MHz, 298 K):** δ 35.42 (m, P*C*H$_2$), 31.58, 29.02 (2 × m, P*C*H$_3$). **^{31}P{^{1}H} NMR (C$_6$D$_6$, 243 MHz, 298 K):** δ 68.97 (s). **^{1}H NMR (C$_6$D$_6$, 500 MHz, 334 K):** δ 1.97, 1.12 (2 × s, 24H, PC*H*$_3$), 1.92, 1.72 (2 × m, 8H, PC*H*$_2$), –22.70 (quin., $^2J_{H,P}$ 52.7 Hz, 2H, Mn*H*). **^{31}P{^{1}H} NMR (C$_6$D$_6$, 202 MHz, 334 K):** δ 68.82 (s). **^{1}H NMR (*d*$_8$-toluene, 500 MHz, 189 K):** δ 1.94, 1.15 (2 × s, 24H, PC*H*$_3$), 1.94, 1.73 (2 × m, 8H, PC*H*$_2$), –22.59 (quin., $^2J_{H,P}$ 51.2 Hz, 2H, Mn*H*). **^{13}C{^{1}H} NMR (*d*$_8$-toluene, 126 MHz, 189 K):** δ 34.75 (m, P*C*H$_2$), 30.83, 28.74 (2 × s, P*C*H$_3$). **^{31}P{^{1}H} NMR (*d*$_8$-toluene, 202 MHz, 189 K):** δ 69.80, 69.61 (2 × s, 4P). ***cis*,*cis*-6: ^{1}H NMR (C$_6$D$_6$, 600 MHz, 298 K):** δ –12.13 (br. s, 2H, Mn*H*). **^{1}H NMR (C$_6$D$_6$, 500 MHz, 334 K):** δ –12.16 (br. app. quintet, $^2J_{H,P}$ 21.8 Hz, 2H, Mn*H*). **^{1}H NMR (*d*$_8$-toluene, 500 MHz, 189 K):** δ –11.54, –11.81, –12.09, –12.27 (4 × m; relative intensities are 2.1 : 1.4 : 1.4 : 1, Mn*H*). ***cis*,*trans*-6: ^{1}H NMR (C$_6$D$_6$, 600 MHz, 298 K):** δ –10.93 (quin., $^2J_{H,P}$ 24.1 Hz, 1H, Mn*H*), –20.96 (quin., $^2J_{H,P}$ 52.6 Hz, 1H, Mn*H*). **^{1}H NMR (C$_6$D$_6$, 500 MHz, 334 K):** δ –11.01 (br. s, 1H, Mn*H*), –20.94 (br. s, 1H, Mn*H*). **^{1}H NMR (*d*$_8$-toluene, 500 MHz, 189 K):** δ –10.78 (m, 1H, Mn*H*), –21.02 (quin., $^2J_{H,P}$ 50.5 Hz, 1H, Mn*H*). **Signals not definitively assigned to *cis*,*cis*-6 or *cis*,*trans*-6**: **^{1}H NMR (C$_6$D$_6$, 600 MHz, 298 K):** δ 2.20, 1.48, 1.28, 0.90, 0.77 (5 × br. s), 2.07, 2.04, 1.92, 1.24, 1.21, 1.11, 1.03 (7 × s). **^{13}C{^{1}H} NMR (C$_6$D$_6$, 151 MHz, 298 K):** δ 33.51, 25.33 (2 × br. s), 25.98 (s). **^{31}P{^{1}H} NMR (C$_6$D$_6$, 243 MHz, 298 K):** δ 76.01, 72.33, 67.58, 65.54, 63.36, 61.44 (6 × br. s; broad and substantially lower intensity features not included). **^{31}P{^{1}H} NMR (C$_6$D$_6$, 202 MHz, 334 K):** δ 72.01, 65.18 (2 × br. s). **^{1}H NMR (*d*$_8$-toluene, 500 MHz, 189 K):** δ 2.51 (d, $J_{H,P}$ 3.2 Hz), 2.40 (d, $^2J_{H,P}$ 6.0 Hz), 2.13 (d, $^2J_{H,P}$ 4.3 Hz), 2.10, 1.78, 1.24, 0.98, 0.97, 0.96, 0.94, 0.89, 0.59 (9 × s), 1.83 (d, $J_{H,P}$ 5.5 Hz), 1.81, 1.75 (2 × d, $J_{H,P}$ 5.6 Hz), 1.52 (d, $J_{H,P}$ 5.2 Hz), 1.50 (d, $J_{H,P}$ 5.1 Hz), 1.08 (d, $J_{H,P}$ 3.1 Hz), 1.03, 0.92, 0.72, 0.71, 0.70 (5 × m), 0.86 (d, $J_{H,P}$ 2.1 Hz). **^{13}C{^{1}H} NMR (*d*$_8$-toluene, 126 MHz, 189 K):** δ 26.98, 26.08, 25.08 (3 × m), 24.51, 24.15, 23.40, 23.18, 21.35, 14.67 (6 × s). **^{31}P{^{1}H} NMR (*d*$_8$-toluene, 202 MHz, 189 K):** δ 77.91, 75.39, 73.34, 64.73, 63.97, 62.02, 61.12, 60.74 (8 × br. s), 69.01, 65.51, 62.82 (3 × m). **Anal.** found (calcd): C, 36.94 (36.72); H, 8.54 (8.47).

X-ray quality crystals of [O{^{n}BuGe=MnH(dmpe)$_2$}] (7). Approximately 10 mg of [(dmpe)$_2$MnH(=GeH^{n}Bu)] (**3b**) was dissolved in a limiting amount of hexamethyldisiloxane, followed by addition of a large excess (a few drops) of H$_3$Ge^{n}Bu contaminated with a small amount of an impurity {^{1}H NMR: 5.54 ppm (t, $^3J_{H,H}$ = 2.0 Hz)} tentatively identified as O(^{n}BuGeH$_2$)$_2$}.¶¶ The solution was maintained at –30 °C, and orange X-ray quality crystals of **7** were obtained. Attempts to isolate **7** on a preparative scale were unsuccessful. Addition of the same contaminated batch of H$_3$Ge^{n}Bu to [(dmpe)$_2$MnH(=GePh$_2$)] (**2a**), [(dmpe)$_2$MnH(=GeEt$_2$)] (**2b**) or [(dmpe)$_2$MnH(=GeH^{n}Bu)] (**3b**) in C$_6$D$_6$ afforded the expected mixture of **3b**, **4b**, and **5b**, accompanied by a very low-intensity Mn*H* peak at –12.89 ppm (quin., $^2J_{H,P}$ 51.5 Hz) which may be due to **7**; for the solution formed from **2b**, removal of volatiles *in vacuo* afforded a solution composed primarily of **3b** but with the peak associated with **7** having an intensity approximately 4% of that of the **3b** Mn*H* environment.

Conflicts of interest

There are no conflicts to declare.

Acknowledgements

D.J.H.E. and I.V.B. thank NSERC of Canada for Discovery Grants, and D.J.H.E. thanks the Digital Research Alliance of Canada (previously Compute Canada) for a 2020 Resources for Research Groups (RRG) grant. We are also grateful to Dr. Yurij Mozharivskyj for access to his X-ray diffractometer and Dr. Paul Ayers for helpful advice regarding DFT calculations.

Notes and references

‡ Attempts to obtain single crystals of **4a-b** or **5a-b** by maintaining solutions containing **4a-b** and **5a-b** (generated by mixing **2a-b** or **3b** with a large excess of H$_3$GePh or H$_3$Ge^{n}Bu in various solvents) at –30 °C only afforded powders. However, when a batch of H$_3$Ge^{n}Bu contaminated with a small amount of an impurity tentatively identified as O(GeH$_2$^{n}Bu)$_2$ was used, an X-ray crystal structure of the bimetallic bis(germylene) complex [O{^{n}BuGe=MnH(dmpe)$_2$}] (**7**) was obtained (see experimental section and ESI for details).

§ For **5a**, NMR spectroscopy did not allow conclusive assignment of the terminal Ge*H* ^{1}H NMR signals (those in the germyl vs the hydrogermane ligand). These signals were assigned by analogy to those in **5b** (which were conclusively assigned).

¶ The HSiR$_3$ ligands in previously reported *trans*-[(dmpe)$_2$MnH(HSiR$_3$)] complexes feature Si–H Mayer bond orders of 0.30-0.34, and were described as nonclassical hydrosilane ligands resulting from significant but incomplete hydrosilane oxidative addition.[52] The HGeR$_3$ ligands in **5a-b** could described similarly.

†† For the reaction involving H$_3$GePh, H$_2$GePh$_2$ was identified in the reaction mixture by comparison to the ^{1}H NMR spectrum of pure diphenylgermane. For the reaction involving H$_3$Ge^{n}Bu, H$_2$Ge^{n}Bu$_2$ was tentatively identified from the ^{1}H NMR spectrum of the reaction mixture based on the presence of a quintet ($^3J_{H,H}$ = 3.1 Hz, C$_6$D$_6$) at 3.90 ppm (cf. the Ge*H* environment in the ^{1}H NMR spectrum of H$_2$GeEt$_2$ is a quintet at 3.85 ppm with coupling to the four α hydrocarbyl hydrogens of 3.2 Hz).

‡‡ This information was measured using 2D NMR spectroscopy, 1D TOCSY NMR spectroscopy, or $^{1}H\{^{31}P\}$ NMR spectroscopy.

§§ In the $^{1}H\{^{31}P\}$ NMR spectrum, these signals are doublets with $^{2}J_{H,H}$ = 6.7 Hz.

¶¶ For comparison, $O(MeGeH_2)_2$ has been reported to give rise to a Ge*H* environment at 5.28 ppm with $^{3}J_{H,H}$ of 2.9 Hz in CCl_4.[93]

1. A. G. Massey, A. J. Park and F. G. A. Stone, *J. Am. Chem. Soc.*, 1963, **85**, 2021.
2. A. N. Nesmeyanov, K. N. Anisimov, N. E. Kolobova and A. B. Antonova, *Izv. Akad. Nauk SSSR, Ser. Khim.*, 1966, 160-162.
3. A. N. Nesmeyanov, G. G. Dvoryantseva, T. N. Ul'yanova, N. E. Kolobova, K. N. Anisimov and A. B. Antonova, *Izv. Akad. Nauk SSSR, Ser. Khim.*, 1967, 2241-2246.
4. K. N. Anisimov, N. E. Kolobova, A. B. Antonova and B. V. Bezborodov, *Izv. Akad. Nauk SSSR, Ser. Khim.*, 1968, 202-204.
5. M. D. Curtis and R. C. Job, *J. Am. Chem. Soc.*, 1972, **94**, 2153-2155.
6. J. P. Collman, J. K. Hoyano and D. W. Murphy, *J. Am. Chem. Soc.*, 1973, **95**, 3424-3425.
7. R. C. Job and M. D. Curtis, *Inorg. Chem.*, 1973, **12**, 2514-2519.
8. K. Triplett and M. D. Curtis, *J. Am. Chem. Soc.*, 1975, **97**, 5747-5751.
9. H. Behrens, M. Moll, P. Merbach and K. H. Trummer, *Z. Naturforsch., B: Anorg. Chem., Org. Chem.*, 1986, **41B**, 845-851.
10. W. A. Herrmann, H. J. Kneuper and E. Herdtweck, *Chem. Ber.*, 1989, **122**, 433-436.
11. D. Lei and M. J. Hampden-Smith, *J. Chem. Soc., Chem. Commun.*, 1989, 1211-1213.
12. D. Lei, M. J. Hampden-Smith, E. N. Duesler and J. C. Huffman, *Inorg. Chem.*, 1990, **29**, 795-798.
13. D. Lei, M. J. Hampden-Smith, J. W. Garvey and J. C. Huffman, *J. Chem. Soc., Dalton Trans.*, 1991, 2449-2457.
14. J. Brugos, J. A. Cabeza, P. García-Álvarez and E. Pérez-Carreño, *Organometallics*, 2018, **37**, 1507-1514.
15. M. Veith, M. Olbrich, M. Notzel, C. Klein, L. Stahl and V. Huch, *CSD Communication*, 1999.
16. D. Agustin, G. Rima, H. Gornitzka and J. Barrau, *Inorg. Chem.*, 2000, **39**, 5492-5495.
17. L. W. Pineda, V. Jancik, J. F. Colunga-Valladares, H. W. Roesky, A. Hofmeister and J. Magull, *Organometallics*, 2006, **25**, 2381-2383.
18. J. A. Cabeza, P. García-Álvarez, E. Pérez-Carreño and D. Polo, *Inorg. Chem.*, 2014, **53**, 8735-8741.
19. J. A. Cabeza, P. García-Álvarez, R. Gobetto, L. González-Álvarez, C. Nervi, E. Pérez-Carreño and D. Polo, *Organometallics*, 2016, **35**, 1761-1770.
20. P. Jutzi and W. Steiner, *Chem. Ber.*, 1976, **109**, 3473-3479.
21. W. R. Cullen, F. W. B. Einstein, R. K. Pomeroy and P. L. Vogel, *Inorg. Chem.*, 1975, **14**, 3017-3020.
22. W. Gäde and E. Weiss, *Chem. Ber.*, 1981, **114**, 2399-2404.
23. B. Schiemenz and G. Huttner, *Chem. ber.*, 1994, **127**, 2129-2133.
24. G. Albertin, S. Antoniutti and J. Castro, *J. Organomet. Chem.*, 2012, **696**, 4191-4201.
25. S. Wolf, S. Wei, W. Klopper, S. Dehnen and C. Feldmann, *Inorg. Chem.*, 2020, **59**, 12895-12902.
26. B. T. Kilbourn, T. L. Blundell and H. M. Powell, *Chem. Commun. (London)*, 1965, 444-445.
27. F. Carré, G. Cerveau, E. Colomer and R. J. P. Corriu, *J. Organomet. Chem.*, 1982, **229**, 257-273.
28. D. J. Brauer and R. Eujen, *Organometallics*, 1983, **2**, 263-267.
29. W.-P. Leung, C.-W. So, K.-W. Kan, H.-S. Chan and T. C. W. Mak, *Inorg. Chem.*, 2005, **44**, 7286-7288.
30. W. Gäde and E. Weiss, *J. Organomet. Chem.*, 1981, **213**, 451-460.
31. D. Melzer and E. Weiss, *J. Organomet. Chem.*, 1984, **263**, 67-73.
32. J. D. Korp, I. Bernal, R. Hörlein, R. Serrano and W. A. Herrmann, *Chem. Ber.*, 1985, **118**, 340-347.
33. N. M. Kostić and R. F. Fenske, *J. Organomet. Chem.*, 1982, **233**, 337-351.
34. E. T. Ouellette, A. Carpentier, I. Joseph Brackbill, T. D. Lohrey, I. Douair, L. Maron, R. G. Bergman and J. Arnold, *Dalton Trans.*, 2021, **50**, 2083-2092.
35. P. Ghana, M. I. Arz, U. Chakraborty, G. Schnakenburg and A. C. Filippou, *J. Am. Chem. Soc.*, 2018, **140**, 7187-7198.
36. R. C. Handford, P. W. Smith and T. D. Tilley, *J. Am. Chem. Soc.*, 2019, **141**, 8769-8772.
37. J. S. Price, D. J. H. Emslie and J. F. Britten, *Angew. Chem., Int. Ed.*, 2017, **56**, 6223-6227.
38. J. S. Price, D. J. H. Emslie, I. Vargas-Baca and J. F. Britten, *Organometallics*, 2018, **37**, 3010-3023.
39. G. S. Girolami, G. Wilkinson, M. Thornton-Pett and M. B. Hursthouse, *J. Am. Chem. Soc.*, 1983, **105**, 6752-6753.
40. G. S. Girolami, C. G. Howard, G. Wilkinson, H. M. Dawes, M. Thornton-Pett, M. Motevalli and M. B. Hursthouse, *J. Chem. Soc., Dalton Trans.*, 1985, 921-929.
41. T. P. Dhungana, H. Hashimoto and H. Tobita, *Dalton Trans.*, 2017, **46**, 8167-8179.
42. K. Nagata, H. Omura, M. Matsuoka, H. Tobita and H. Hashimoto, *Organometallics*, 2023, **42**, 1131-1138.
43. A. Shinohara, J. McBee and T. D. Tilley, *Inorg. Chem.*, 2009, **48**, 8081-8083.
44. T. P. Dhungana, H. Hashimoto, M. Ray and H. Tobita, *Organometallics*, 2020, **39**, 4350-4361.
45. H. Hashimoto, T. Tsubota, T. Fukuda and H. Tobita, *Chem. Lett.*, 2009, **38**, 1196-1197.

46. M. Widemann, S. Jeggle, M. Auer, K. Eichele, H. Schubert, C. P. Sindlinger and L. Wesemann, *Chem. Sci.*, 2022, **13**, 3999-4009.
47. P. G. Hayes, R. Waterman, P. B. Glaser and T. D. Tilley, *Organometallics*, 2009, **28**, 5082-5089.
48. M. E. Fasulo and T. D. Tilley, *Chem. Commun. (Cambridge, U. K.)*, 2012, **48**, 7690-7692.
49. M. C. Lipke, F. Neumeyer and T. D. Tilley, *J. Am. Chem. Soc.*, 2014, **136**, 6092-6102.
50. J. S. Price and D. J. H. Emslie, *Chem. Sci.*, 2019, **10**, 10853-10869.
51. John R. Rumble, ed., CRC Handbook of Chemistry and Physics, 103rd Edition (Internet Version 2022), CRC Press/Taylor & Francis, Boca Raton, FL.
52. J. S. Price, D. J. H. Emslie and B. Berno, *Organometallics*, 2019, **38**, 2347-2362.
53. J. L. Vincent, S. Luo, B. L. Scott, R. Butcher, C. J. Unkefer, C. J. Burns, G. J. Kubas, A. Lledós, F. Maseras and J. Tomàs, *Organometallics*, 2003, **22**, 5307-5323.
54. N. Zhang, R. S. Sherbo, G. S. Bindra, D. Zhu and P. H. M. Budzelaar, *Organometallics*, 2017, **36**, 4123-4135.
55. A. C. Filippou, K. W. Stumpf, O. Chernov and G. Schnakenburg, *CSD Communication*, 2011.
56. A. C. Filippou, K. W. Stumpf, O. Chernov and G. Schnakenburg, *CSD Communication*, 2011.
57. Y. G. Budnikova, T. V. Gryaznova, O. G. Sinyashin, S. A. Katsyuba, T. P. Gryaznova and M. P. Egorov, *J. Organomet. Chem.*, 2007, **692**, 4067-4072.
58. F. M. Bickelhaupt and E. J. Baerends, in *Reviews in Computational Chemistry*, eds. D. B. Boyd and K. B. Lipkowitz, Wiley-VCH, New York, 2000, pp. 1-86.
59. T. Ziegler and A. Rauk, *Inorg. Chem.*, 1979, **18**, 1755-1759.
60. T. Ziegler and A. Rauk, *Inorg. Chem.*, 1979, **18**, 1558-1565.
61. A. Kramida, Y. Ralchenko, J. Reader, and NIST ASD Team (2022). NIST Atomic Spectra Database (version 5.10). https://physics.nist.gov/asd [Fri Jul 7 2023].
62. V. Y. Lee, *Eur. J. Inorg. Chem.*, 2022, e202200175.
63. A. G. Orpen and N. G. Connelly, *Organometallics*, 1990, **9**, 1206.
64. J. E. B. B. J. Burger, in *Experimental Organometallic Chemistry - A Practicum in Synthesis and Characterization*, American Chemical Society, Washington, D.C., 1987, vol. 357, pp. 79-98.
65. K. V. Zaitsev, I. P. Gloriozov, Y. F. Oprunenko, E. K. Lermontova and A. V. Churakov, *J. Organomet. Chem.*, 2019, **897**, 217-227.
66. R. K. Harris, E. D. Becker, S. M. Cabral de Menezes, R. Goodfellow and P. Granger, *Pure Appl. Chem.*, 2001, **73**, 1795-1818.
67. G. M. Sheldrick, *Acta Crystallogr., Sect. A: Found. Adv.*, 2015, **71**, 3-8.
68. G. M. Sheldrick, *Acta Crystallogr., Sect. C: Struct. Chem.*, 2015, **71**, 3-8.
69. O. V. Dolomanov, L. J. Bourhis, R. J. Gildea, J. A. K. Howard and H. Puschmann, *J. Appl. Crystallogr.*, 2009, **42**, 339-341.
70. ADF 2020.102, SCM, Theoretical Chemistry, Vrije Universiteit, Amsterdam, The Netherlands, http://www.scm.com.
71. G. te Velde, F. M. Bickelhaupt, E. J. Baerends, C. Fonseca Guerra, S. J. A. Van Gisbergen, J. G. Snijders and T. Ziegler, *J. Comput. Chem.*, 2001, **22**, 931-967.
72. J. P. Perdew, K. Burke and M. Ernzerhof, *Phys. Rev. Lett.*, 1996, **77**, 3865-3868.
73. E. van Lenthe, E. J. Baerends and J. G. Snijders, *J. Chem. Phys.*, 1993, **99**, 4597-4610.
74. E. van Lenthe, E. J. Baerends and J. G. Snijders, *J. Chem. Phys.*, 1994, **101**, 9783-9792.
75. E. van Lenthe, A. Ehlers and E.-J. Baerends, *J. Chem. Phys.*, 1999, **110**, 8943-8953.
76. E. van Lenthe, J. G. Snijders and E. J. Baerends, *J. Chem. Phys.*, 1996, **105**, 6505-6516.
77. E. van Lenthe, R. van Leeuwen, E. J. Baerends and J. G. Snijders, *Int. J. Quantum Chem.*, 1996, **57**, 281-293.
78. S. Grimme, J. Antony, S. Ehrlich and H. Krieg, *J. Chem. Phys.*, 2010, **132**, 154104.
79. S. Grimme, S. Ehrlich and L. Goerigk, *J. Comput. Chem.*, 2011, **32**, 1456-1465.
80. A. D. Becke, *J. Chem. Phys.*, 1988, **88**, 2547-2553.
81. M. Franchini, P. H. T. Philipsen and L. Visscher, *J. Comput. Chem.*, 2013, **34**, 1819-1827.
82. A. Bérces, R. M. Dickson, L. Y. Fan, H. Jacobsen, D. Swerhone and T. Ziegler, *Comput. Phys. Commun.*, 1997, **100**, 247-262.
83. H. Jacobsen, A. Bérces, D. P. Swerhone and T. Ziegler, *Comput. Phys. Commun.*, 1997, **100**, 263-276.
84. S. K. Wolff, *Int. J. Quantum Chem.*, 2005, **104**, 645-659.
85. M. Ernzerhof and G. E. Scuseria, *J. Chem. Phys.*, 1999, **110**, 5029-5036.
86. S. Grimme, *J. Comput. Chem.*, 2004, **25**, 1463-1473.
87. T. Ziegler and A. Rauk, *Inorg. Chem.*, 1979, **18**, 1755-1759.
88. T. Ziegler and A. Rauk, *Inorg. Chem.*, 1979, **18**, 1558-1565.
89. M. Mitoraj and A. Michalak, *Organometallics*, 2007, **26**, 6576-6580.
90. A. Michalak, M. Mitoraj and T. Ziegler, *J. Phys. Chem. A*, 2008, **112**, 1933-1939.
91. M. P. Mitoraj, A. Michalak and T. Ziegler, *Organometallics*, 2009, **28**, 3727-3733.
92. M. P. Mitoraj, A. Michalak and T. Ziegler, *J. Chem. Theory Comput.*, 2009, **5**, 962-975.
93. J. E. Drake, B. M. Glavinčevski, H. E. Henderson and R. T. Hemmings, *Can. J. Chem.*, 1978, **56**, 465-472.